Polyhedron 33 (2012) 235–251

Contents lists available at SciVerse ScienceDirect

Polyhedron

journal homepage: www.elsevier.com/locate/poly

Dinuclear and polynuclear dioxomolybdenum(VI) Schiff base complexes: Synthesis, structural elucidation, spectroscopic characterization, electrochemistry and catalytic property

Ngui Khiong Ngan *, Kong Mun Lo, Chee Seng Richard Wong

Department of Chemistry, University of Malaya, 50603 Kuala Lumpur, Malaysia

ARTICLE INFO

Article history:
Received 17 October 2011
Accepted 18 November 2011
Available online 17 December 2011

Keywords:
Crystal structure
Dioxomolybdenum(VI)
Hydrogen bonding
Supramolecules
Schiff base
Oxidation of alcohol

ABSTRACT

Several new binuclear and polynuclear dioxomolybdenum(VI) Schiff base complexes have been synthesized. The reaction of bis(acetylacetonato)dioxomolybdenum with 5-dichlorosalicylaldehyde 4-ethylthiosemicarbazide (**L1**/**L2**) in the presence of 4,4′-bipyridine (4,4′-bpy) or 4,4′-bipyridine *N*,*N*′-dioxide (4,4′-dpdo) gave a binuclear *cis*-dioxomolybdenum complex **[(MoO$_2$)$_2$L$_2$(D-D)]**, in which the bidentate ligand, 4,4′-bipyridine or 4,4′-bipyridine *N*,*N*′-dioxide (**D-D**), formed a bridge between the two molybdenum atoms. A second type of dinuclear dioxomolybdenum(VI) Schiff base complex, **[(MoO$_2$)$_2$L′D$_2$]**, was formed by the reaction of bis(acetylacetonato)dioxomolybdenum with 1,4-bis(3-ethoxy-salicylaldehyde carbohydrazonato)butane (**L′**) in the presence of ethanol or hexamethylphosphoramide (**D**). In this case, the two molybdenum atoms are not bridged directly by a bidentate ligand, but are coordinated at each end to the O,N,O donor atoms of the symmetrical hexadentate Schiff base ligand. The syntheses of polynuclear dioxomolybdenum(VI) **[(MoO$_2$)L′(D-D)]$_n$** complexes were achieved by the reaction of the second type of dinuclear dioxomolybdenum(VI) complex, **[(MoO$_2$)$_2$L′D$_2$]**, with the bidentate ligand 4,4′-bipyridine (**D-D**). These complexes were characterized by elemental analysis, electronic spectra, IR, ^{1}H and ^{13}C NMR spectroscopies, thermogravimetric analysis and cyclic voltammetry. An X-ray study shows that each molybdenum site in the dinuclear and polynuclear complexes adopts an octahedron geometry. The dioxomolybdenum(VI) complexes show catalytic activity for the oxidation of alcohols with H_2O_2 as an oxidant.

1. Introduction

Molybdenum chemistry has been widely investigated in recent years. Subsequently, various ligands with different donor properties, such as hydrazone and thiosemicarbazone ligands, have been subjected to coordination with dioxomolybdenum to produce complexes which serve as catalysts in biological and industrial processes. Hydrazone (*ONO*) and thiosemicarbazone (*ONS*) tridentate Schiff base ligands are of particular interest as they offer a labile site in mononuclear dioxomolybdenum(VI) complexes which allows binding and displacement of different substrate molecules. Moreover, these complexes have also attracted research interest for their possible antitumor [1], antifungal [2] and antiviral [3] properties. From a supramolecular architectural point of view, hydrazone ligands can stabilize the overall molecular framework by inducing intra- and intermolecular hydrogen bonding interactions through the amido nitrogen.

Hydrogen bonding is the most reliable directional interaction in supramolecular construction. For such reasons, for more than a decade, chemists have been actively engaged in the study of the structure, spectroscopic, electrochemistry and oxo-transferase properties of oxomolybdenum complexes [4–12]. At present, there are plenty of mononuclear dioxomolybdenum(VI) complexes reported, but systems with binuclear complexes based on bis(hydrazone) and thiosemicarbazone ligands are rare [13]. Koo et al. have reported binuclear complexes bridged by 4,4′-dipyridyl *N*,*N*′-dioxide, but no definite structures were elucidated [14,15].

As a part of our study on molybdenum complexes, three types of complexes with different nuclearity have been synthesized and characterized spectroscopically. The X-ray crystal structures of the complexes exhibit various intriguing supramolecular architectures. In this report, we are also concerned with and investigate the catalytic behavior of dinuclear and polynuclear dioxomolybdenum(VI) complexes towards the oxidation of alcohol.

2. Experimental

2.1. General procedures

All the reagents and solvents used in the synthesis were procured commercially and used without subsequent purification.

* Corresponding author.
E-mail address: nicky_ngan@hotmail.com (N.K. Ngan).

0277-5387/$ - see front matter © 2011 Elsevier Ltd. All rights reserved.
doi:10.1016/j.poly.2011.11.057

The starting material, bis(acetylacetonato)dioxomolybdenum(VI), $[MoO_2(acac)_2]$, was prepared as described in the literature [16].

2.2. Physical measurements

The melting points of the compounds were determined on a Melt-Temp apparatus and were uncorrected. Elemental analysis was performed at the in-house microanalytical laboratory using a Perkin-Elmer 2400 Series II CHNS/O System. IR spectra were recorded in the range 4000–400 cm^{-1} using Perkin-Elmer Spectrum 2000 FT-IR and Perkin-Elmer Spectrum RX1 FT-IR spectrophotometers. The samples were prepared either as nujol mulls or KBr pellets. ^1H and ^{13}C NMR spectra of the ligands and the complexes were measured in DMSO-d_6 at ambient temperature on a JEOL Lambda 400 FT-NMR SYSTEM spectrometer operating at 399.65 MHz for ^1H and at 100.40 MHz for ^{13}C NMR on an ECA 400 MHz NMR spectrometer. Electronic absorption spectral measurements of the ligands and the complexes in DMF were measured using a Shimadzu-1650-PC-UV–Vis spectrophotometer and the samples were scanned from 200 to 800 nm. Thermal analysis (TGA) of the complexes was carried out by heating in nitrogen gas at a rate of 20 °C per minute on a Perkin-Elmer TGA-4000 thermo balance. DSC curves were obtained at a heating rate of 20 °C per minute in N_2 atmosphere over the temperature range 50–350 °C on a Perkin-Elmer DSC 6 series. Cyclic voltammetry was carried out using a Methrohm Autolab B.V. model. The measurements were done in DMF solution containing 0.1 M TEAP as a supporting electrolyte and a 5×10^{-4} M complex solution was deoxygenated by bubbling with nitrogen gas before use. The working, counter and reference electrodes used were Pt wire, platinum coil and SCE, respectively. The X-ray crystallographic intensity data were measured using Mo Kα radiation (graphite crystal monochromator, λ = 0.71069 Å). The data collection was collected at 296 K on a Bruker APEX II with a CCD area-detector X-ray diffractometer. The structures were solved by the direct method with the SHELXS97 [17] program and refined on F^2 by full-matrix least-squares methods with anisotropic non-hydrogen atoms. Crystal data are given in Table 3 and selected bond distances and angles are reported in Tables 4–6.

2.3. Synthesis of 5-chlorosalicylaldehyde 2-ethylthiosemicarbazone (*L1*)

0.156 g (1.0 mmol) of 5-chlorosalicylaldehyde in 20 ml methanol was added to 20 ml of 0.120 g (1.0 mmol) of 2-ethylthiosemicarbazide. The solution mixture was refluxed with vigorous stirring for 2 h. The resulting solution was then filtered and allowed to stand at room temperature, during which time a pale yellow solid was formed. The precipitate was filtered, washed with methanol and air-dried. The ligand was used without further purification. M.p.: 150–153 °C, (0.23 g, 68%). *Anal.* Calc. for $C_{10}H_{12}N_3OClS$: C, 46.69; H, 4.67; N, 16.34; S, 12.40. Found: C, 47.01; H, 4.17; N, 15.95; S, 12.32%; IR(KBr) (ν_{max}/cm^{-1}): 3301 (m, NH), 3128 (m, OH), 1602 (m, C=N), 1537 (m, C_{ar}–O), 1269 (s, C=S); ^1H NMR (DMSO-d_6, ppm): 11.38 (1H, NH), 10.33 (1H, –OH), 8.62 (1H, HC=N), 6.85–7.23 (aromatic proton), 1.15 (5H, $-OCH_2CH_3$); ^{13}C NMR (DMSO-d_6, ppm): 178.51 (C=S), 159.89 (C=N), 118.23, 122.70, 123.97, 126.00, 131.17, 139.67 (aromatic ring), 24.67, 33.14 ($-CH_2CH_3$).

2.4. Synthesis of 3,5-dichlorosalicylaldehyde 2-ethylthiosemicarbazone (*L2*)

0.191 g (1.0 mmol) of 3,5-dichlorosalicylaldehyde in 20 ml methanol was added to a 20 ml hot stirring methanolic solution of 0.119 g (1.0 mmol) of 2-ethylthiosemicarbazide. The solution mixture was refluxed for 2 h. The yellowish reaction mixture became cloudy. The resulting solution was then filtered and the filtrate was allowed to stand at room temperature, whereupon a yellow precipitate was formed. The precipitate was washed with methanol and dried in air. The ligand was used without further purification. M.p.: 123–125 °C, (0.15 g, 63%). *Anal.* Calc. for $C_{10}H_{12}N_3OSCl_2$: C, 40.96; H, 4.10; N, 16.38; S, 10.92. Found: C, 41.07; H, 4.23; N, 16.44; S, 11.21%; IR(KBr) (ν_{max}/cm^{-1}): 3438 (m, NH), 3190 (m, OH), 1607 (m, C=N), 1540 (m, C_{ar}–O), 1263 (s, C=S); ^1H NMR (DMSO-d_6, ppm): 11.57 (1H, NH), 10.68 (1H, –OH), 8.45 (1H, HC=N), 6.77–7.63 (aromatic proton), 1.15 (5H, $-CH_2CH_3$); ^{13}C NMR (DMSO-d_6, ppm): 178.51 (C=S), 159.89 (C=N), 120.43, 127.07, 133.60, 135.00, 138.17, 139.67 (aromatic ring), 25.56, 34.41 ($-CH_2CH_3$).

2.5. Preparation of the ligands

2.5.1. General procedures

All the Schiff base ligands **L3**–**L5** were prepared by the condensation reactions of 3-ethoxylsalicylaldehyde, 3,5-dichlorosalicylaldehyde and 4-hydroxsalicylaldehyde with adipic acid dihydrazide in a 1:2 ratio, respectively, as shown in Scheme 1.

Table 1
Thermogravimetric analysis of the complexes.

Comp.	Temp. range (°C)	Weight loss observed (calculated) (%)	DSC_{max} (°C)	Molecules removed	End residue
C1	(a) 200–270	(a) 15.66 (14.82)	242 (−)	(a) Bipyridine	MoO_2
	(b) 270–870	(b) 72.00 (75.69)		(b) 2 Tridentate ligands	
C2	(a) 220–270	(a) 14.32 (16.27)	234 (−)	(a) Bipyridine N dioxide	MoO_2
	(b) 270–700	(b) 56.54 (60.92)		(b) 2 Tridentate ligands	
C3	(a) 150–200	(a) 13.44 (11.30)	175 (+)	(a) 2 Ethanol	–
	(b) 200–270	(b) 11.35 (11.30)	229 (−)	(b) 2 $-OC_2H_5$	
	(c) 270–730	(c) 42.12 (44.25)		(c) Hexadentate ligands	
	(d) 730–900	(d) 27.78 (31.44)		(d) $2MoO_2$	
C4	(a) 170–200	(a) 10.53 (10.62)	160 (+)	(a) 2 Ethanol	–
	(b) 300–350	(b) 18.00 (16.40)	206 (+)	(b) 4-Cl	
	(c) 350–620	(c) 40.57 (41.57)	252 (−)	(c) Hexadentate ligands	
	(d) 620–870	(d) 28.00 (27.45)		(d) $2MoO_2$	
C5	(a) 100–400	(a) 42.46 (41.20)	170 (+)	(a) Hexadentate ligands	MoO_2
	(b) 400–850	(b) 30.52 (32.96)		(b) 2 HMPA	
C6	(a) 150–270	(a) 19.76 (16.82)	164 (+), 189 (+)	(a) 2 DMF	MoO_2
	(b) 270–870	(b) 52.18 (53.88)	251 (−)	(b) Hexadentate ligands	
C7	(a) 200–280	(a) 18.13 (16.50)	251 (+)	(a) Bipyridine	MoO
	(b) 300–874	(b) 72.48 (73.32)	270 (−)	(b) Ligands	

Table 2
UV–Vis wavelengths for the ligands and the complexes.

Compounds	λ_{max} (nm)
L1	347, 315, 262
L2	351, 317, 268
L3	291, 251
L4	338, 302, 291
L5	338, 303, 292
C1	346, 315, 267
C2	405, 347, 270
C3	404, 290, 247
C4	398, 322, 286
C5	387, 290, 248
C6	387, 336, 248
C7	393, 309, 268

Table 3a
Cyclic voltammmetry data.

Compounds	E_{pc}/V (I_{pc}/μA)	E_{pa}/V (I_{pa}/μA)
L1	−0.42 (1.28)	–
L2	−0.36 (0.35)	–
L3	−0.37 (3.90)	−0.28 (5.35)
L4	−0.38 (0.13)	−0.28 (5.09)
L5	−0.49 (0.26)	
C1	−0.39 (8.14), −0.94 (2.21)	−0.21 (1.91)
C1	−0.40 (0.23), −0.94 (3.42)	–
C3	−0.38 (0.14), −0.86 (3.45),	−0.29 (5.32)
C4	−0.38 (7.77), −0.85 (3.12)	−0.28 (1.81)
C5	−0.38 (0.11), −0.83 (2.12)	−0.28 (5.64)
C6	−0.38 (0.15), −0.85 (3.68)	−0.29 (5.89)
C7	−0.40 (4.79), −0.86 (1.18)	−0.25 (1.38)

*2.5.2. Synthesis of 1,4-bis(3-ethoxysalicylaldehyde carbohydrazonato)butane (**L3**)*

0.332 g (2.0 mmol) of 3-ethoxysalicylaldehyde in 40 ml ethanol was added to 30 ml of a hot ethanolic solution of 0.174 g (1.0 mmol) adipic acid dihydrazide. The solution mixture was refluxed with vigorous stirring for 2 h. The resulting yellow solution was then cooled to room temperature. Upon standing at room temperature for 2 days, the yellow precipitate that formed was filtered, washed with ethanol and dried in air. The ligand was used without further purification. M.p.: 158–160 °C, (0.23 g, 61%). *Anal.* Calc. for $C_{24}H_{30}N_4O_4$: C, 65.75; H, 6.85; N, 12.76. Found: C, 66.18; H, 6.70; N, 13.12%; IR(KBr) (ν_{max}/cm^{-1}): 3591 (s, OH), 3439, 3287 (m, N–H), 1660 (s, C=O), 1590 (m, C=N), 1555 (m, C_{ar}–O); ^{1}H NMR (DMSO-d_6, ppm): 11.58 (–OH), 11.2, 10.90 (NH), 8.30 (HC=N), 6.74–7.20 (aromatic), 3.17, 1.21 (–OCH_2CH_3), 3.41 (–CH_2CH_2); ^{13}C NMR (DMSO-d_6, ppm): 154.70 (C=N), 167.82 (C=O), 113.71, 115.22, 119.20, 137.43, 148.93, 154.70 (aromatic), 102.17, 108.62 (–C_2H_4), 64.34, 14.75 (–OCH_2CH_3).

*2.5.3. Synthesis of 1,4-bis(3,5-dichlorosalicylaldehyde carbohydrazonato)butane (**L4**)*

0.382 g (2.0 mmol) of 3,5-dichlorosalicylaldehyde in 40 ml ethanol was added to 30 ml of a hot ethanolic solution of 0.174 g (1.0 mmol) adipic acid dihydrazide. The solution mixture was refluxed with vigorous stirring for 2 h. The resulting yellow solution was then cooled to room temperature. Upon standing at room temperature for 2 days, the yellow precipitate that formed was filtered, washed with ethanol and dried in air. The ligand was used without further purification. M.p.: 240–242 °C, (0.22 g, 48%). *Anal.* Calc. for $C_{20}H_{18}N_4O_4Cl_2$: C, 53.45; H, 4.01; N, 12.47. Found: C, 53.12; H, 4.09; N, 11.87%; IR(KBr) (ν_{max}/cm^{-1}): 3443 (s, OH), 3295, 3253 (m, N–H), 1681 (s, C=O), 1608 (m, C=N), 1537 (m, C_{ar}–O); ^{1}H NMR (DMSO-d_6, ppm): 11.95 (–OH), 11.47 (NH), 8.24 (HC=N), 6.89–7.48 (aromatic), 3.42 (–CH_2CH_2); ^{13}C NMR (DMSO-d_6, ppm): 152.60 (C=N), 169.23 (C=O), 123.36, 128.83, 130.54, 140.77, 145.77, 151.27 (aromatic), 121.20, 121.84 (–C_2H_4).

*2.5.4. Synthesis of 1,4-bis(4-hydroxysalicylaldehyde carbohydrazonato)butane (**L5**)*

0.336 g (2.0 mmol) of 4-hydroxysalicylaldehyde in 40 ml ethanol was added to 30 ml of a hot ethanolic solution of 0.174 g (1.0 mmol) adipic acid dihydrazide. The solution mixture was refluxed with vigorous stirring for 2 h. The resulting pale pink solution was then cooled to room temperature. Upon standing at room temperature for 2 days, the white precipitate that formed was filtered, washed with ethanol and dried in air. The ligand was used without further purification. M.p.: 258–260 °C, (0.21 g, 34%). *Anal.* Calc. for $C_{20}H_{22}N_4O_6$: C, 57.97; H, 5.31; N, 13.53. Found: C, 58.54; H, 5.22; N, 13.27%; IR(KBr) (ν_{max}/cm^{-1}): 3264 (s, OH), 1681 (s, C=O), 1608 (m, C=N), 1520 (m, C_{ar}–O); ^{1}H NMR (DMSO-d_6, ppm): 11.40, 11.02 (–OH), 10.18 (NH), 8.19 (HC=N), 6.26–7.37 (aromatic), 3.49 (–CH_2CH_2); ^{13}C NMR (DMSO-d_6, ppm): 159.25 (C=N), 173.19 (C=O), 110.40, 111.42, 128.76, 131.22, 143.24, 147.44 (aromatic), 102.38, 107.79 (–C_2H_4).

2.6. Preparation of the dinuclear–dimolybdenum(VI) complexes

*2.6.1. Synthesis of bis(5-chlorosalicylaldehyde 2-ethylthiosemicarbazonato) 4,4-bipyridyl dinuclear dioxomolybdenum(VI) (**C1**)*

0.328 g (1.0 mmol) of $MoO_2(acac)_2$ in 40 ml of ethanol was mixed with 40 ml of 0.258 g (1.0 mmol) 5-chlorosalicylaldehyde 2-ethylthiosemicarbazone. The resulting solution was refluxed with vigorous stirring for 1 h. Then 0.078 g of 4,4-bipyridine in 10 ml of ethanol was added to the mixture and the heating was continued for another hour. After leaving the solution for 1 week at room temperature, dark brown crystals were formed. The product was filtered, washed with ethanol and air-dried. M.p.: 222–224 °C, (0.25 g, 34%). *Anal.* Calc. for $C_{30}H_{28}O_6N_8S_2Cl_2Mo_2$: C, 39.00; H, 3.03; N, 12.13; S, 6.93. Found: C, 40.12; H, 3.33; N, 11.67; S, 7.25%; IR(KBr) (ν_{max}/cm^{-1}): 3336 (m, N–H), 1603 (m, C=N), 1546 (m, C_{ar}–O), 1003, 1063, 1579 (4,4′-bpy), 927, 897 (Mo=O); ^{1}H NMR (DMSO-d_6, ppm): 8.75 (HC=N), 7.85, 8.53, 8.72 (4,4′-bpy); 6.87–7.72 (aromatic); ^{13}C NMR (DMSO-d_6, ppm): 177.22 (C–S), 157.34 (C=N), 150.44, 122.64, 121.34 (4,4′-bpy), 119.75, 123.89, 128.67, 131.87, 132.00, 144.58 (aromatic).

*2.6.2. Synthesis of bis(3,5-dichlorosalicylaldehyde 2-ethylthiosemicarbazonato) 4,4bipyridyl N,N′-dioxide dinuclear dioxomolybdenum(VI) (**C2**)*

0.328 g (1.0 mmol) of $MoO_2(acac)_2$ in 40 ml of ethanol was mixed with 40 ml of 0.293 g (1.0 mmol) of 3,5-dichlorosalicylaldehyde 2-ethylthiosemicarbazone. The resulting solution was refluxed with vigorous stirring for 1 h. Then 0.093 g of 4,4-bipyridine *N,N′*-dioxide in 10 ml of ethanol solution was added to the mixture and the heating is continued for another hour. After leaving the solution for 1 week at room temperature, dark brown crystals were formed. The product was filtered, washed with ethanol and dried in air. M.p.: 212–214 °C, (0.32 g, 43%). *Anal.* Calc. for $C_{30}H_{26}O_8N_8S_2Cl_4Mo_2$: C, 35.16; H, 2.54; N, 10.94; S, 6.25. Found: C, 36.53; H, 2.75; N, 11.11; S, 5.39%; IR(KBr) (ν_{max}/cm^{-1}): 3234 (m, N–H), 1586 (m, C=N), 1549 (m, C_{ar}–O), 1212 (s, C–S), 823, 834 (m, N–O), 922, 891 (Mo=O);

Table 3b
Crystallographic data and structure refinement parameters for compounds **C1**, **C2**, **C3**, **C4**, **C5**, **C6** and **C7**.

Compounds	**C1**	**C2**	**C3**	**C4**	**C5**	**C6**	**C7**
Chemical formula	$C_{30}H_{28}Cl_2N_8O_6S_2Mo_2$	$C_{30}H_{24}Cl_4N_8O_8S_2Mo_2$	$C_{28}H_{38}N_4O_{12}Mo_2$	$C_{24}H_{26}Cl_4N_4O_{12}Mo_2$	$C_{36}H_{62}N_{10}O_{12}P_2Mo_2$	$C_{30}H_{40}N_6O_{12}Mo_2$	$C_{16}H_{17}O_6N_3Mo$
M_r	923.52	1022.31	814.50	864.15	1080	868.56	443.27
Crystal color, habit	red, block	red, block	brown, block	brown, block	yellow, block	yellow, block	red, block
Crystal size (mm)	0.40 × 0.30 × 0.30	0.25 × 0.20 × 0.10	0.45 × 0.45 × 0.30	0.40 × 0.30 × 0.20	0.40 × 0.20 × 0.08	0.27 × 0.14 × 0.10	0.40 × 0.30 × 0.20
Crystal system	monoclinic	triclinic	monoclinic	monoclinic	triclinic	triclinic	monoclinic
Space group	$P21/n$	$P\bar{1}$	$P\ 2(1)/c$	$C2/c$	$P\bar{1}$	$P\bar{1}$	$P2_1/c$
Unit cell dimensions							
a (Å)	12.5483(2)	9.0527(2)	8.8304(4)	20.5338(2)	8.2462(4)	8.36030(10)	10.04650(10)
b (Å)	11.93150(10)	9.2002(2)	12.5291(5)	14.64580(10)	8.3898(4)	10.18100(10)	14.5139(2)
c (Å)	23.2930(3)	12.3846(2)	14.4997(6)	13.24770(10)	18.9782(10)	11.94300(10)	12.6256(2)
α (°)	90.00	71.9720(10)	90.00	90.00	86.238(2)	94.2080(10)	90
β (°)	100.9000(10)	72.5420(10)	99.696(2)	129.51(2)	83.245(2)	107.7120(10)	113.0800(10)
γ (°)	90.00	89.1080(10)	90.00	90.00	68.532(2)	112.4400(10)	90
V (Å^3)	3424.51(8)	932.25(3)	1581.29(12)	3073.74(4)	1213.05(10)	874.054(15)	1693.63(4)
Z	4	1	2	4	1	1	4
T (K)	296(2)	296(2)	296(2)	296(2)	296(2)	296(2)	100(2)
D_{calc} (g cm^{-3})	1.791	1.825	1.711	1.863	1.480	1.650	1.738
μ(Mo Kα) (mm^{-1})	1.067	1.132	0.862	1.224	0.648	0.787	0.814
Absorption correction	multiscan	multiscan	multiscan	multiscan	multiscan	multiscan	multiscan
T_{min}	0.688	0.762	0.685	0.641	0.857	0.876	0.746
T_{max}	0.726	0.893	0.772	0.777	0.950	0.924	0.850
$F(000)$	1848	510	828	2216	558	442	896
Total data	33860	8863	13584	14499	10168	8361	14197
Unique data	8497	4225	3625	3536	4715	3984	3324
R_{int}	0.0190	0.0197	0.0251	0.0182	0.0193	0.0133	0.0331
Observed data [$I > 2\sigma(I)$]	7911	3823	3304	3322	4524	3874	2945
Ranges of h, k, l	−16,16; −15,15; −31,31	−11,11; −11,11; −16,16	−11,11; −16,16; −18,17	−26,26; −19,19; −17,17	−10,10; −10,10; −23,21	−10,10; −12,13; −15,15	−12,12; −17,17; −15,15
Number of parameters	453	249	214	204	287	229	238
R_1	0.0194	0.0291	0.0333	0.0193	0.0321	0.0207	0.0429
wR_2	0.0502	0.0965	0.0866	0.0538	0.0969	0.0602	0.1163
S	1.081	1.095	1.133	0.980	1.167	1.160	1.121
$\Delta\rho_{max}$ (e Å^{-3})	0.454	0.957	0.589	0.534	1.369	0.463	0.896
$\Delta\rho_{min}$ (e Å^{-3})	−0.419	−0.555	−0.805	−0.461	−0.732	−0.452	−0.824

^{1}H NMR (DMSO-d_6, ppm): 8.75 (HC═N), 6.87–7.72 (aromatic), 7.85, 8.53, 8.72 (4,4′-bpy); ^{13}C NMR (DMSO-d_6, ppm): 174.98 (C–S), 155.28 (C═N), 129.11, 121.37 (4,4′-bpy *N*,*N*′-dioxide), 118.57, 120.58, 125.49, 132.70, 149.43 (aromatic).

2.6.3. Synthesis of 1,4-bis(3-ethoxysalicylaldehyde carbohydrazonato)butane ethanol dinuclear dioxomolybdenum(VI) (*C3*)

0.656 g (2.0 mmol) of $MoO_2(acac)_2$ in 40 ml of ethanol was mixed with 40 ml of 0.438 g (1.0 mmol) of 1,4-bis(3-ethoxysalicylaldehyde carbohydrazonone)butane. The resulting orange solution was then heated to reflux for 2 h. After leaving the solution overnight at room temperature, light brown crystals were formed. The product was filtered, washed with ethanol and dried in air. M.p.: 135–137 °C, (0.47 g, 53%). *Anal.* Calc. for $C_{28}H_{38}O_{12}N_4Mo_2$: C, 41.28; H, 4.67; N, 6.88. Found: C, 42.36; H, 4.12; N, 7.23%; IR(KBr) (ν_{max}/cm^{-1}): 1614 (m, C═N), 1562 (m, C_{ar}–O), 1250 (s, C_{enolic}–O), 942, 911 (Mo═O); ^{1}H NMR (DMSO-d_6, ppm): 8.71 (HC═N), 6.93–7.23 (aromatic), 3.21, 1.64 (–OCH_2CH_3), 4.06 (–CH_2CH_2); ^{13}C NMR (DMSO-d_6, ppm): 175.00 (C═O), 155.24 (C═N), 118.57, 120.54, 121.32, 125.46, 147.63, 149.23 (aromatic), 64.36, 56.05 (O–CH_2CH_3).

2.6.4. Synthesis of 1,4-bis(3,5-dichlorosalicylaldehyde carbohydrazonato)butane ethanol dinuclear dioxomolybdenum(VI) (*C4*)

0.656 g (2.0 mmol) of $MoO_2(acac)_2$ in 40 ml of ethanol was mixed with 40 ml of 0.449 g (1.0 mmol) of 1,4-bis(3-ethoxysalicylaldehyde carbohydrazonone)butane. The resulting orange solution was then heated to reflux for 2 h. After leaving the solution for 4 days at room temperature, dark orange crystals were formed. The product was filtered, washed with ethanol and dried in air. M.p.: 310–312 °C, (0.14 g, 23%). *Anal.* Calc. for $C_{24}H_{28}O_{10}N_4Cl_4Mo_2$: C, 33.26; H, 3.23; N, 6.47. Found: C, 32.54; H, 3.49; N, 7.29%; IR(KBr) (ν_{max}/cm^{-1}): 1613 (m, C═N), 1539 (m, C_{ar}–O), 1267 (s, C_{enolic}–O), 943, 916 (Mo═O); ^{1}H NMR (DMSO-d_6, ppm): 8.77 (HC═N), 6.93–7.83 (aromatic), 3.89 (–CH_2CH_2–); ^{13}C NMR (DMSO-d_6, ppm): 176.00 (C═O), 154.04 (C═N), 122.23, 123.87, 124.28, 131.96, 133.25, 153.43 (aromatic), 107.51 (–CH_2CH_2–).

2.6.5. Synthesis of 1,4-bis(3-ethoxysalicylaldehyde carbohydrazonato)butane hexamethylphosphoramide dinuclear dioxomolybdenum(VI) (*C5*)

0.656 g (2.0 mmol) of $MoO_2(acac)_2$ in 40 ml of ethanol was mixed with 40 ml of 0.438 g (1.0 mmol) of 1,4-bis(3-ethoxysalicylaldehyde carbohydrazonone)butane. The resulting orange solution was then heated to reflux for 1 h. A few drops of hexamethylphosphoramide were added to the solution and an immediate orange color precipitate was formed. A sufficient amount of dimethylformamide was added to the mixture until the precipitate was completely dissolved. The resulting orange solution was left at room temperature for 5 days, during which time a yellow solid was formed. Recrystallization of the resulting orange solid from dimethylformamide with the slow evaporation technique afforded yellow colored crystals. The product was filtered, washed with ethanol and dried in air. M.p.: 172–174 °C (0.37 g, 44%). *Anal.* Calc. for $C_{32}H_{62}O_{12}N_{10}P_2Mo_2$: C, 37.21; H, 6.01; N, 13.57. Found: C, 36.74; H, 6.42; N, 13.23%; IR(KBr) (ν_{max}/cm^{-1}): 1621 (m, C═N), 1566 (m, C_{ar}–

Table 4
Bond lengths (Å) and bond angles (°) for **C1**.

Mo(1)–O(2)	1.7078(12)	Mo(2)–O(6)	1.7054(12)
Mo(1)–O(3)	1.7109(12)	Mo(2)–O(5)	1.7119(12)
Mo(1)–O(1)	1.9476(12)	Mo(2)–O(4)	1.9512(12)
Mo(1)–N(1)	2.2921(14)	Mo(2)–N(5)	2.2696(14)
Mo(1)–S(1)	2.4123(4)	Mo(2)–S(2)	2.4245(4)
Mo(1)–N(4)	2.4565(14)	Mo(2)–N(8)	2.4270(14)
N(2)–C(8)	1.307(2)	N(5)–C(22)	1.296(2)
N(2)–N(1)	1.3849(19)	N(5)–N(6)	1.3791(19)
C(8)–S(1)	1.7615(17)	C(23)–S(2)	1.7618(17)
C(1)–O(1)	1.339(2)	C(16)–O(4)	1.344(2)
N(1)–C(7)	1.297(2)	N(6)–C(23)	1.308(2)
O(6)–Mo(2)–O(5)	106.26(6)	O(2)–Mo(1)–O(3)	105.93(6)
O(6)–Mo(2)–O(4)	98.00(6)	O(2)–Mo(1)–O(1)	105.03(6)
O(5)–Mo(2)–O(4)	106.30(6)	O(3)–Mo(1)–O(1)	100.16(6)
O(6)–Mo(2)–N(5)	89.33(6)	O(2)–Mo(1)–N(1)	160.39(6)
O(5)–Mo(2)–N(5)	161.45(6)	O(3)–Mo(1)–N(1)	91.14(5)
O(4)–Mo(2)–N(5)	80.73(5)	O(1)–Mo(1)–N(1)	80.74(5)
O(6)–Mo(2)–S(2)	101.26(5)	O(2)–Mo(1)–S(1)	91.21(5)
O(5)–Mo(2)–S(2)	90.71(5)	O(3)–Mo(1)–S(1)	99.71(4)
O(4)–Mo(2)–S(2)	149.54(4)	O(1)–Mo(1)–S(1)	149.65(4)
N(5)–Mo(2)–S(2)	76.14(4)	N(1)–Mo(1)–S(1)	76.16(4)
O(6)–Mo(2)–N(8)	170.45(5)	O(2)–Mo(1)–N(4)	80.50(5)
O(5)–Mo(2)–N(8)	83.02(5)	O(3)–Mo(1)–N(4)	173.54(5)
O(4)–Mo(2)–N(8)	76.82(5)	O(1)–Mo(1)–N(4)	77.31(5)
N(5)–Mo(2)–N(8)	81.96(5)	N(1)–Mo(1)–N(4)	82.61(5)
S(2)–Mo(2)–N(8)	80.52(3)	S(1)–Mo(1)–N(4)	80.42(3)

O), 1260 (s, C_{enolic}–O), 1131 (s, P=O), 928, 899 (Mo=O); ^{1}H NMR (DMSO-d_6, ppm): 2.50 and 2.52 (HMPA), 3.85, (3H, O–CH_3), 4.08 (5H, O–C_2H_5), 6.93–7.80 (aromatic), 8.49 (1H, HC=N); ^{13}C NMR (DMSO-d_6, ppm): 36.56, 36.60 (HMPA), 65.60 (O–C_2H_5), 159.44 (C=N), 170.06 (C=O), 112.75, 118.00, 119.58, 120.45, 121.06, 121.28, 125.45, 129.19, 132.54, 148.63, 151.49, 153.82 (12C, aromatic).

2.6.6. Synthesis of 1,4-bis(3-ethoxysalicylaldehyde carbohydrazonato)butane dimethylformamide dinuclear dioxomolybdenum(VI) (**C6**)

0.656 g (2.0 mmol) of $MoO_2(acac)_2$ in 40 ml of ethanol was mixed with 40 ml of 0.438 g (1.0 mmol) of 1,4-bis(3-ethoxysalicylaldehyde carbohydrazonone)butane. The resulting orange solution mixture was then heated to reflux for 1 h. A few drops of dimethylformamide were added to the solution and the heating was continued for another hour. After leaving the solution for 1 week at room temperature, yellow crystals were formed. The product was filtered, washed with ethanol and dried in air. M.p.: 125–127 °C, (0.29 g, 22%). *Anal.* Calc. for $C_{30}H_{40}O_{12}N_6Mo_2$: C, 41.47; H, 4.61; N, 9.68. Found: C, 40.88; H, 5.04; N, 10.23%; IR(KBr) (ν_{max}/cm^{-1}): 1618 (m, C=N), 1563 (m, C_{ar}–O), 1247 (s, C_{enolic}–O), 737 (s, HC=O_{DMF}), 930, 899 (Mo=O); ^{1}H NMR (DMSO-d_6, ppm): 2.89 and 2.73 (DMF), 7.01–7.95 (aromatic), 8.72 (1H, HC=N); ^{13}C NMR (DMSO-d_6, ppm): 174.80 (C=O_{DMF}), 155.11 (C=N), 162.21 (C=O_{enol}), 118.43, 120.41, 121.19, 125.33, 148.00, 149.28 (aromatic ring), 30.66 and 35.67 (DMF).

Table 5
Bond lengths (Å) for the complexes.

	C2	C3	C4	C5	C6	C7
Mo(1)–O(2)	1.712(2)	1.707(2)	1.6968(12)	1.713(2)	1.7169(13)	1.729(3)
Mo(1)–O(3)	1.709(2)	1.692(2)	1.7009(13)	1.700(2)	1.7032(13)	1.696(3)
Mo(1)–O(1)	1.954(2)	1.923(2)	1.9312(12)	1.929(2)	1.9412(13)	1.933(3)
Mo(1)–N(1)	2.288(3)	2.234(2)	2.2591(13)	2.243(3)	2.2242(16)	2.217(4)
Mo(1)–S(1)/O(4)	2.4165(8)	2.0257(19)	2.0161(12)	2.022(2)	2.0143(13)	2.001(3)
Mo(1)–N(3/4)/O(5/6)	2.297(2)	2.327(2)	2.2786(14)	2.205(2)	2.2849(13)	2.392(4)
C(1)–O(1)	1.329(4)	1.343(3)	1.327(2)	1.341(4)	1.350(2)	1.359(5)
N(2)–C(8/9/10)	1.314(4)	1.296(4)	1.303(2)	1.296(5)	1.296(2)	1.291(5)
N(2)–N(1)	1.377(3)	1.411(3)	1.4040(18)	1.404(4)	1.403(2)	1.404(5)
C(8/10)–S(1)/O(4)	1.753(3)	1.313(3)	1.3118(19)	1.318(4)	1.324(2)	1.315(5)
N(1)–C(7/8/9)	1.301(4)	1.286(3)	1.286(2)	1.286(5)	1.285(2)	1.292(5)

2.6.7. Synthesis of octaoxo-di{bis(4-hydroxysalicylaldehyde) butane dihydrazonato} 4,4′-bipyridy tetranuclear dioxomolybdenum(VI) (**C7**)

0.656 g (2.0 mmol) of $MoO_2(acac)_2$ in 40 ml of methanol was mixed with 40 ml of 0.414 g (1.0 mmol) of 1,4-bis(4-hydroxysalicylaldehyde carbohydrazonone)butane. The resulting red solution was heated to reflux for 1 h, then 0.078 g of 4,4-bipyridine in 10 ml of methanol solution was added to the mixture and the heating was continued for another hour. After leaving the solution for 1 week at room temperature, red crystals were formed. The product was filtered, washed with methanol and dried in air. M.p.: 232–235 °C, (0.22 g, 43%). *Anal.* Calc. for $C_{15}H_{17}N_3O_5Mo$: C, 43.37; H, 4.09; N, 10.12. Found: C, 43.88; H, 4.18; N, 10.23%; IR(KBr) (ν_{max}/cm^{-1}): 3256 (m, –OH), 1609 (m, C=N), 1567 (m, C_{ar}–O), 1230 (s, C_{enolic}–O), 1010, 1069 and 1548 (4,4′-bpy), 926, 883 (Mo=O); ^{1}H NMR (DMSO-d_6, ppm): 10.51 (–OH), 8.70 (1H, HC=N), 7.80, 8.53 (4,4′-bpy), 6.21–7.40 (aromatic); ^{13}C NMR (DMSO-d_6, ppm): 155.39 (C=N), 164.55 (C=O_{enol}), 105.06, 110.57, 112.82, 136.19, 144.95, 161.65 (aromatic ring), 150.44, 121.89 (4,4′-bpy), 49.12 (CH_3OH).

3. Result and discussion

3.1. Synthesis

A series of mononuclear, dinuclear and polynuclear oxomolybdenum(VI) complexes containing either tridentate dianionic or hexadentate tetraanionic donating ligands and a neutral monodentate solvent molecule were prepared as shown in the overall reaction synthetic pathway, Scheme 2.

In the preparation of the tridentate dianionic (ONO/ONS) ligand and hexadentate tetraanionic (ONO–ONO) ligands, different substituted salicylaldehydes were reacted with monohydrazide and adipic acid dihydrazide compounds, respectively, to produce mononucleating and binucleating ligands. The reaction of bis(acetylacetonato)dioxomolybdenum(VI) and the tridentate dianionic ligands, using methanol as a refluxing medium, afforded mononuclear oxomolybdenum(VI) complexes with ONO and ONS donor ligands system. These tridentate ligands were used for complexation as the complexes formed leave a labile coordination site that can be used for substrate binding. In the case of mononuclear dioxomolybdenum(VI) complexes of the *–ONS* ligand system, an effort has been made to displace the alcohol molecule by using 4,4-bipyridine and 4,4-bipyridine *N,N′*-dioxide. This reaction managed to produce a series of dinuclear oxomolybdenum(VI) complexes, in which two Mo atoms were interconnected by the bidentate ligands. Different types of dinuclear oxomolybdenum(VI) complexes were formed by the reaction of the hexadentate tetraanionic ligand with bis(acetylacetonato)dioxomolybdenum(VI) in the presence of ethanol. In this case, the two molybdenum atoms are not bridged directly by a bidentate ligand, but are coordinated at each end by the O,N,O donor atoms of the symmetrical hexadentate Schiff base ligand. The reaction proceeded by displacing the ethanol molecule in the first case using a monodentate ligand to yield another dinuclear oxomolybdenum(VI) complex of the same series. To complete the synthetic work, the preparation of tetranuclear dioxomolybdenum(VI) complexes has been carried out by combining the dinuclear dioxomolybdenum(VI) complex of the

Table 6
Bond angles (°) for the complexes.

	C2	C3	C4	C5	C6	C7
O(3)–Mo(1)–N(1)	89.24(10)	93.48(9)	93.55(5)	90.43(11)	90.73(6)	90.13(15)
O(1)–Mo(1)–N(1)	81.71(9)	81.59(8)	81.42(5)	81.82(10)	81.08(5)	81.75(12)
O(2)–Mo(1)–N(1)	161.49(10)	158.69(9)	159.60(6)	162.16(11)	160.92(6)	159.64(14)
O(2)–Mo(1)–S(1)/O(4)	88.83(8)	97.27(9)	99.00(5)	97.54(10)	94.85(6)	93.70(13)
O(3)–Mo(1)–S(1)/O(4)	101.96(8)	97.44(9)	94.84(5)	94.78(11)	100.42(6)	98.18(15)
O(1)–Mo(1)–S(1)/O(4)	150.58(7)	149.73(8)	150.32(5)	150.57(10)	147.41(6)	149.12(13)
N(1)–Mo(1)–S(1)/O(4)	75.75(7)	71.29(8)	71.59(5)	71.80(10)	71.48(5)	71.65(12)
O(2)–Mo(1)–N(4)/O(4/5/6)	84.96(9)	84.98(9)	84.97(5)	87.97(10)	84.92(6)	84.20(14)
O(3)–Mo(1)–N(4)/O(4/5/6)	169.14(10)	168.72(9)	168.99(5)	165.98(10)	169.92(6)	169.42(15)
O(1)–Mo(1)–N(4)/O(4/5/6)	74.86(9)	81.92(8)	81.78(5)	83.33(10)	78.99(5)	80.61(12)
N(1)–Mo(1)–N(4)/O(4/5/6)	83.28(8)	75.26(8)	75.66(5)	75.97(9)	79.52(5)	79.32(13)
S(1)/O(4)–Mo(1)–N(4)/O(4/5/6)	83.85(6)	78.47(8)	79.80(5)	77.91(9)	79.03(5)	79.32(12)
O(2)–Mo(1)–O(3)	104.17(11)	106.04(11)	105.47(6)	104.98(12)	105.14(7)	106.28(16)
O(2)–Mo(1)–O(1)	108.88(10)	103.76(9)	102.36(5)	104.29(11)	106.82(6)	107.35(13)
O(3)–Mo(1)–O(1)	96.34(10)	97.38(10)	99.03(6)	98.30(11)	97.10(6)	97.27(14)

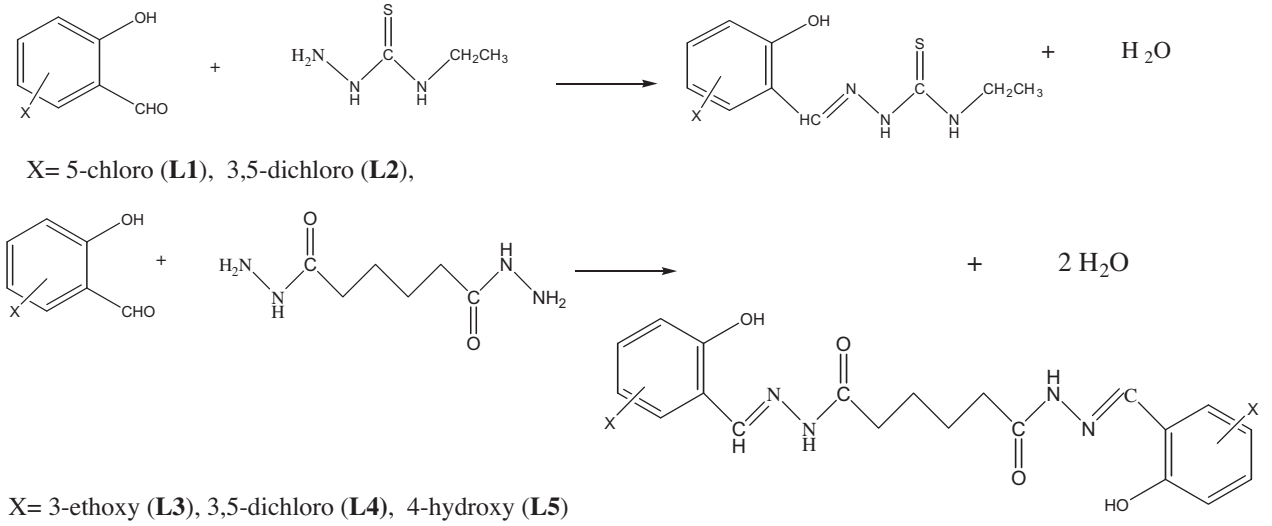

Scheme 1. Preparation of the ligands.

hexadentate tetraanionic ligand system with the 4,4-bipyridine bidentate ligand, and the attempt was successful. Two units of dinuclear dioxomolybdenum were bridged by 4,4-bipyridine and the adjacent molecules were joined together, forming a polymeric chain through hydrogen bonding interactions between the hexadentate ligands.

3.2. Infrared spectra spectroscopic description

The IR spectra of the complexes **C1**–**C7** were analyzed in comparison with that of the free ligands, **L1**–**L5**. The precursor complex of $MoO_2(acac)_2$ has two sharp bands at 934 and 906 cm^{-1}, which are related to the symmetrical and anti-symmetrical stretching of *cis*-MoO_2^{2+}, respectively. These bands in the complexes **C1**–**C7** appear between 897 and 941 cm^{-1}, indicating that the MoO_2^{2+} symmetrical and anti-symmetrical stretching vibrations are independent of the electron donating and accepting capacity of the ligands [18,19]. These data also indicate the presence of a *cis*-MoO_2 structure as a *trans*-MoO_2 unit would normally show one $\nu_{Mo=O}$ band due to the asymmetry stretch [20]. It is revealed from the IR absorption frequencies for the $\nu_{Mo=O}$ band of the Mo(VI) oxo-complexes that the coordination of the neutral bidentate N–N donor ligands (4,4-bipyridine/4,4-bipyridine *N*,*N*′-dioxide) has the effect of lowering the Mo=O stretching frequency [21], as is shown in **C1**, **C2** and **C7**. In the IR spectra of the free thiosemicarbazone and hydrazone ligands, imine ($\nu_{C=N}$) stretching bands appeared between 1590 and 1610 cm^{-1}, but for the complexes, the characteristic imine bands were observed at higher stretching frequencies ranges, namely 1610–1620 cm^{-1}, indicating the coordination of the imine nitrogen atom to the metal center. The coordination of 4,4-bipyridine is characterized by the ring breathing mode of pyridine, which occurs at 990 cm^{-1} in free pyridine [22]. The slight increase on chelation in the frequency of the pyridine breathing vibration (1003 cm^{-1}) for **C1** can be attributed to coordination from the pyridine nitrogen to the metal ion. The IR spectrum of **C2** exhibits absorption bands at 823 and 834 cm^{-1} which are assigned as N–O stretching. The free pyridine N–oxide exhibits a band at 1234 cm^{-1} [23]. The N–O stretching frequency, which is lowered upon coordination, is attributed to the weakening of the bond by the reduction of the electron density i the N–O bond and the loss of the double bond character of the N–O bond when the oxygen atom coordinates to the d^0 metal ion [24,25]. In the case of **C5** and **C6**, the bands at 1131 and 737 cm^{-1} are associated with $\nu_{P=O}$ of HMPA and $\nu_{NC=O}$ of DMF solvent molecules.

3.3. ^1H and ^{13}C NMR spectroscopy description

The ^1H and ^{13}C NMR (DMSO-d_6) data of the free ligands and their polynuclear oxomolybdenum(VI) complexes are given in

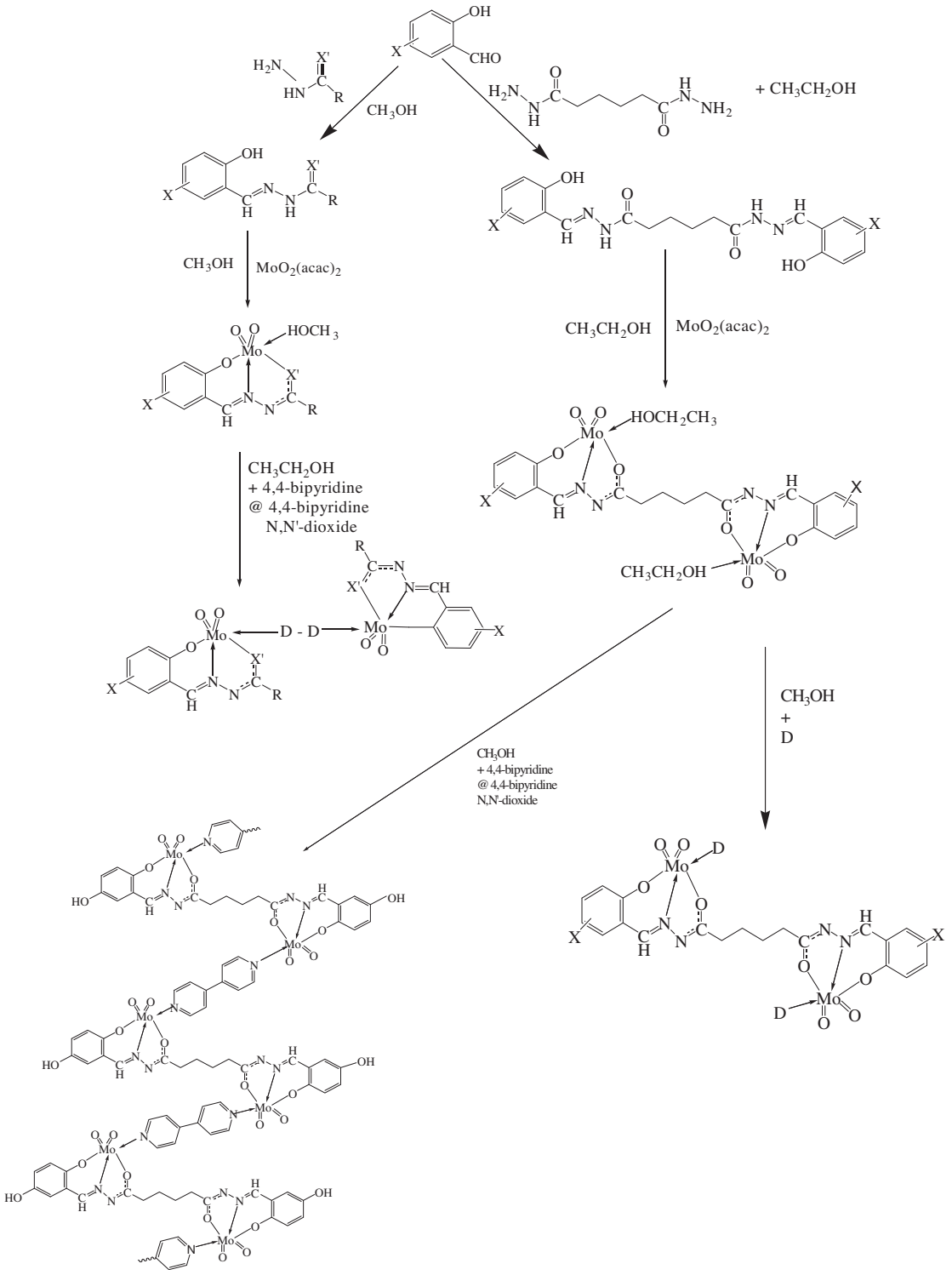

Scheme 2. X = OC_2H_5 or Cl; X′ = S or O; R = NHC_2H_5; **D** = DMF or HMPA; **D-D** = 4,4-bipyridine or 4,4-bipyridine *N*,*N*′-dioxide.

the experimental section. Before the interpretation of the NMR spectra of the complexes is presented, it is appropriate to comment on some points regarding the spectra of the thiosemicarbazone and dihydrazone ligands. The ^{1}H NMR spectra of **L1** and **L2** exhibit a δ-$OH_{phenolic}$ proton resonance at δ 10.33 and 10.68 ppm, and an amide proton, H_{imine}–C=N resonance at δ 8.62 and 8.45 ppm. The broadening of these absorption peaks may occur due to the involvement of the protons in intra- and intermolecular hydrogen bonding interactions [26]. A multiplet due to aromatic protons appears in the δ 6.74–7.63 ppm region in all the five ligands. Furthermore, the signal appearing at δ 3.41 ppm in **L3** is assigned to the proton of the ethylene (–CH_2CH_2–) group. Upon coordination to the Mo atom, the –OH signal in the spectra of the ligands disappears. This suggests that the thiosemicarbazone and dihydrazone ligands are coordinated to the metal center in the enol form, with phenoxyl oxygen atoms. On the other hand, the participation of the

imine nitrogen in complexation is signaled by an appreciable downfield shift of the azomethine proton signal (δ 8.75 ppm). The downfield shift of these signals is attributable to the drainage of the electron density from the nitrogen atom of the azomethine group to the Mo atoms [27]. **C1** and **C2** show a few signals in δ 7.85–8.72 ppm range. These signals are attributed to the protons of the pyridyl rings of the 4,4-bipyridine molecules.

A comparison of ^{13}C NMR spectra of the ligands and complexes revealed several interesting features. The average position of the resonance due to the secondary amido carbonyl carbon atoms is found to have shifted downfield in the complexes. Some new signals which are present in the spectra of **C1**, **C2** and **C7**, but not in the spectra of the ligands, are assigned to the various carbon atoms of 4,4-bipyridine. These signals appeared in the δ 121–154 ppm region. Additionally, it is remarkable to note that **C3**–**C7** show signals at about 110 ppm corresponding to the $-CH_2CH_2-$ group, which appear at 120 ppm in the uncoordinated dihydrazone. The upfield shift of these signals in the complexes indicates that the electron density at the $-CH_2CH_2-$ carbon atoms is increased in the coordinated dihydrazone.

3.4. Thermal properties of the title complexes

Thermal analysis techniques such as thermogravimetry (TGA), differential thermal analysis (DTA) and differential scanning calorimetry (DSC) have been widely applied in studying the thermal behavior of metal complexes. The data enables us to follow a series of structural changes the compounds were subjected to during thermal treatment, and subsequently provides insight pertaining to the thermal stability and thermal decomposition of the compounds in the solid state [28,29].

The TGA analyses of the dinuclear tetraoxomolybdenum(VI) complexes have been carried out in the temperature range 50–900 °C, at a heating rate of 20 °C min^{-1}. The decomposition stages, temperature ranges, found and calculated weight loss percentages, as well as the thermal effects accompanying the changes in the solid complexes on heating are given in Table 1. The thermal behavior of the mononuclear and binuclear molybdenum complexes is different. For different binuclear complexes, the TGA curves show mass losses in a different number of stages, which are due to the removal of the solvent molecules, followed by the departure of the ligands. The area of the endothermic DSC peak corresponds to the melting heat, while the area of the exothermal peak corresponds to the heat of decomposition.

The TGA curve of **C3** shows a mass loss between 150 and 200 °C, corresponding to an endothermic peak temperature at 175 °C, due to the removal of two ethanol molecules. The heat of removal of the ethanol molecules obtained from DSC curve (192.81 J g^{-1}) suggests that the ethanol molecules are loosely attached to the molybdenum center. The second step corresponds to a thermal decomposition between 200 and 270 °C which involves the removal of two $-OCH_2CH_3$ fragments from the dihydrazone ligands. This is supported by the exothermic decomposition temperature peak in DSC curve at 229 °C and the heat of decomposition calculated (−166.42 J g^{-1}). Further removal of the hexadentate ligands occurs at the higher temperature range 270–730 °C according to the TGA curve. The final remaining residue, MoO_2, also undergoes decomposition at 900 °C.

The thermal decomposition of **C5** occurs in two steps. The departure of the hexadentate ligands takes place between 100 and 400 °C with a mass loss of 42.46% (calc. 41.20%). This is supported by the endothermic effect temperature peak in DSC curve at 171 °C and the calculated heat of decomposition (+130.40 J g^{-1}). The next step between 400 and 850 °C corresponds to the removal of two HMPA solvent molecules, leaving MoO_2 as a residue.

The thermal decomposition of both **C1** and **C2** occurs in two steps. The removal of the 4,4-bipyridine and 4,4-bipyridine *N*,*N*′-dioxide begins at 200 °C and ends at 270 °C. It was observed that the decomposition starts without melting. The DSC curves show an exothermic peak temperature at 242 and 234 °C, with $\Delta H = -48.88$ and -320.27 J g^{-1}, respectively. The second stage, which occurs in the temperature range 270–870 °C, corresponds to the decomposition of the two tridentate ligands. The final residue is MoO_2.

The thermal decomposition of **C4** takes place in four steps. Two ethanol molecules are removed followed by the fragmentation of chlorine substituted atoms at the salicylaldehyde rings, observed at 170–200 and 300–350 °C. The third stage is related to the decomposition of the hexadentate ligand, taking place in the temperature range 620–870 °C. The final residue of MoO_2 undergoes further decomposition at 620 °C. The DSC curve shows two endothermic and one exothermic temperature peak at 160, 206 and 252 °C, respectively.

The TGA curve of **C6** shows two stages of thermal decomposition. Two molecules of DMF are eliminated between 150 and 270 °C. The second stage decomposition, which occurs in the temperature range 270–870 °C with a mass loss of 52.18% (calc. 53.88%), accounts for the removal of the hexadentate ligands. The removal of the hexadentate ligands, which occur at 251 °C, required 279 J g^{-1} exothermic heat as shown in the DSC curve. In the case of **C7**, the mass losses (18.13% and 72.48%) that occur in two consecutive complicated transition stages in the temperature ranges 200–280 and 300–874 °C, respectively, are mainly due to the breakage of the 4,4-bipyridine coordinated bond, followed by decomposition of the dihydrazone ligands.

In general, there are differences in the exothermic and endothermic peaks recorded in the DSC curves of the complexes. These differences originate from the packing mode of the complexes. The additional hydrogen bonding interactions in **C1**, **C2**, **C3** and **C7** exert more stability to the crystal structure. More precisely, the decomposition of **C1**, **C2** and **C7** occurred at 200–280 °C and that of **C5** and **C6** at approximately 100 °C. Based on these data, it can be concluded that for the structural transformation in the **C1**, **C2** and **C7** complexes, which are more stable, a larger energy consumption is necessary because of the breakage of a higher number of intermolecular hydrogen bonds. In summary, the thermal decomposition behavior of the complexes can be summarized in Scheme 3.

3.5. Electronic spectral studies

The electronic absorption bands of the ligands and the complexes in 5×10^{-4} M DMF, together with their tentative assignments, are given in Table 2. The absorption bands of the free ligands can be classified into three regions. The absorption region between 250 and 290 nm in the ligands is characteristic for the π to π^* transition of the benzene rings of the ligands. Two absorption bands observed between 290 and 350 nm are probably due to the *n* to π^* transition of the –C═N– and –C═O– or –C═S– moieties of the ligands [30]. The spectra of the complexes show a broad band at ca. 400 nm, which is assignable to a ligand to metal charge transfer (LMCT) due to the promotion of an electron from the highest occupied molecular orbital (HOMO) of the ligand to the lowest unoccupied molecular orbital (LUMO) of molybdenum atom [31]. The electronic spectra of the complexes **C1**–**C7** in DMF display two absorption bands in the 293–312 and 329–355 nm regions. These peaks may be assigned to oxygen to molybdenum and nitrogen to molybdenum charge transfer transitions, respectively [32,33]. The slight change in the λ values within the **L1**–**L5** ligands may be due to their difference in the electron donating property incited by the nature of the substituents. For instance, **L1**, **L2** and **L4** are gradually less electron rich, as a result of the presence of the chlorine atoms. This makes the HOMO of these ligands higher in energy and thus

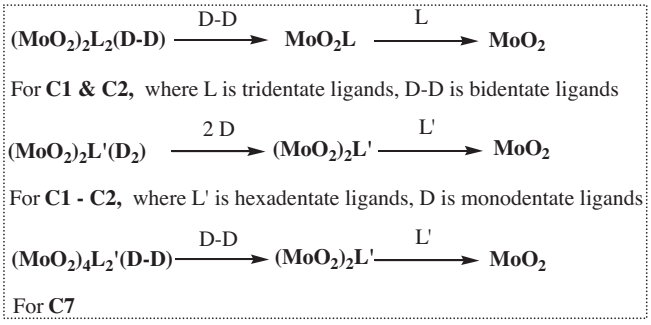

Scheme 3. Thermal decomposition of the dinuclear and polynuclear oxomolybdenum(VI) complexes.

a red shift is experienced [34]. Higher energy bands appearing below 290 nm are due to intra-ligand transitions. The absence of a d–d transition absorption band in the visible region confirms the $4d^0$ electronic configuration of Mo(VI) [35].

3.6. Electrochemical studies

The redox behavior of the ligands and the complexes were examined in DMF solution using cyclic voltammetry at a platinum electrode with 0.1 M tetraethyl ammonium perchlorate (TEAP) as the supporting electrolyte. The CV data is tabulated and selected *I* versus *E* profiles are illustrated in Table 3. From the data, **L3** and **L4** exhibit one irreversible oxidative peak around −0.28 V and one reductive peak at −0.38 V while **L1**, **L2** and **L5** show only one reduction peak from −0.36 to −0.42 V in the cyclic voltammogram recorded in the potential range +2.0 to −1.5 V. The structure as well as the different electron donating properties of the substituent groups in the ligands are probably the leading contributors to the additional anodic oxidative potential in **L3** and **L4**. The CV trace of the complexes displays two irreversible reductive responses within the potential window −0.39 to −0.94V. The reductive wave near −0.39 V in the complexes is due to the effect of the redox behavior of the ligands as the observed values fall in the same region as that for the free ligands. The calculated I_{pa}/I_{pc} ratio = 0.81 and 1.17 for **C1** and **C7**, respectively, indicating that these complexes have a reversible redox property. On the contrary, the other type of dinuclear molybdenum complexes, **C2**–**C6**, show two successive irreversible one electron oxidation and reductions within the range −0.25 to −0.86 V. The emergence of these peaks in the complexes could be assigned to irreversible metal centered and the ligand (bridging)-centered oxidation and reduction processes [36]. The more negative reduction potential of **C2** compared to **C3**–**C7** indicates that the Mo ions in the complexes are much more stable in the higher oxidation state due to the presence of strong and hard donor atoms (N,O) in the Schiff base ligands [37]. In general, CV studies on these dinuclear and polynuclear molybdenum(VI) complexes reveal that the complexes have essentially similar irreversible redox behavior, except for **C1** and **C7** (Fig. 1).

3.7. Crystallographic description of the complexes

The molecular structures and the atom numbering scheme of **C1**–**C7** (Figs. 2–8) show that in **C1** and **C2** the Schiff base ligands behave as tridentate ligands and react with the dioxomolybdenum anion to form a six coordinated molybdenum(VI) complex, in which the bidentate ligand, 4,4′-bipyridine or 4,4′-bipyridine *N*,*N*′-dioxide (**D-D**) forms a bridge between the two molybdenum atoms. In the case of **C3**–**C6**, the two molybdenum atoms are not bridged directly by a bidentate ligand, but are coordinated at each end to the O,N,O donor atoms of the symmetrical hexadentate Schiff base ligand. The reaction of the bidentate ligand, 4,4′-bipyridine, and the symmetrical hexadentate Schiff base ligand with $MoO_2(acac)_2$ yielded a polynuclear Mo(VI) complex, **C7**. All the complexes possess two equivalent halves with a center of inversion, except for **C1** in which the two halves of the dinuclear complex are not crystallographically equivalent but their structural dimensions are closely related.

3.8. Crystallographic description for *C1* and *C2*

As shown in Figs. 2 and 3, the overall geometry of **C1** and **C2** can be regarded as an octahedron, with the equatorial plane defined by the imine nitrogen, phenoxyl oxygen, sulfur atom and one of the terminal oxygen atoms of the dioxomolybdenum unit. The other terminal oxygen and the nitrogen or oxygen atom from the bridging 4,4′-bipyridine or 4,4′-bipyridine *N*,*N*′-dioxide molecules occupy the apical positions. The two oxygen, sulfur, nitrogen and molybdenum atoms are found to be essentially coplanar, in which the molybdenum atom shows a slight shift out (0.2764 and 0.2358 Å) of the basal plane towards the O3 direction. Typical values for the O═Mo═O angles are around 108°, while optimal values for the Mo═O distance lie around 1.70 Å.

The Mo–D (donor atom of solvent) bond length in the dioxomolybdenum(VI) complexes are generally found to be somewhat longer than a normal single bond length due to the consequence of the *trans* effect of $M{=}O_t$ (where O_t is oxo-group *trans* to the $Mo{-}O_{solvent}$ bond). In these cases, the Mo–N(3) distance (2.4566 Å) is longer than that of Mo–O(4) (2.297 Å). This result reveals a rather weak attachment of the 4,4-biypridine ligand compared to the 4,4′-bipyridine *N*,*N*′-dioxide ligand to the MoO_2^{2+} moiety.

A closer look at the crystal structure packing of **C1** shows that the supramolecular rectangular structure of **C1** has been constructed by an intermolecular hydrogen bonding interaction, N7–H7A. . .O3, as shown in Fig. 9 and Table 7. The oxo-group is engaged in the H-bonding interaction with the hydrogen atom attached at the N7 atom from a neighboring molecule, with the result that the chains are interlocked into a two dimensional polymeric network which runs along the *bc* crystallographic plane (Fig. 10). On the contrary, the hydrogen atom from the secondary amine group of one **C2** molecules form a hydrogen bond to a nitrogen atom of the 4,4′-bipyridine of the adjacent **C2** molecule (Fig. 11) and Table 8. This arrangement gives rise to the formation of a one-dimensional helical chain that runs along the diagonal of *ac* crystallographic plane (Fig. 12).

3.9. Crystallographic description for *C3*–*C7*

The structures of **C3**–**C7** consist of $(MoO_2)L$, accompanied by two molecules of donor solvent molecules. Unlike **C1** and **C2**, the octahedral environment around the molybdenum atom comprises of *cis*-Mo═O, imine nitrogen, phenoxyl oxygen and hydroxyl oxygen atoms from the enolized carbonyl group, further supported by monodentate neutral ligands, such as ethanol, DMF and HMPA. The average values for the Mo–O(2)/(3) distance and O═Mo═O angle in these complexes varies slightly in the ranges 1.70–1.72 Å and 104–107°, respectively. On the other hand, a least-square calculation shows that the molybdenum atoms of **C5** deviate the least (0.2118 Å) towards the distal O3, indicating that the deviation is restricted by the presence of the bulky HMPA molecule in the complex. The planarity of this equatorial plane was further corroborated by the close linearity of the O2–Mo–N1 angle of **C5**, 162.16(12)°.

The extended structures of **C3**, **C5**, **C6** and **C7** reveal that the butylene chains of these structures adopt an antiperiplanar or *zigzag* conformation (Figs. 4 and 6–8), except for **C4** in which the

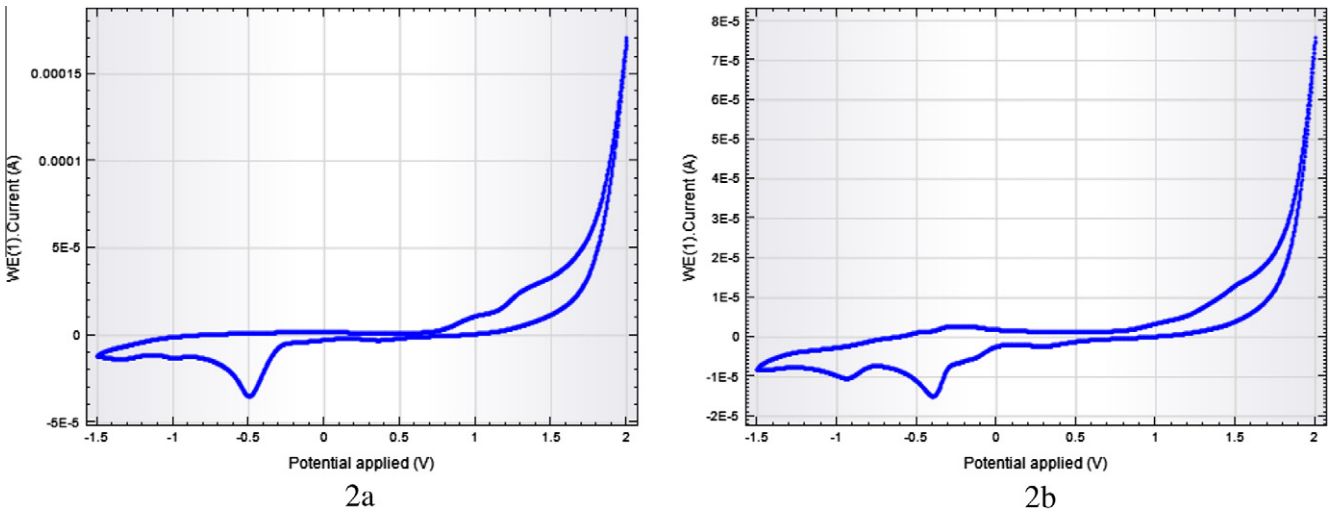

Fig. 1. Cyclic voltammograms for **L1**(2a) and **C1**(2b) – scan rate 100 mV/s.

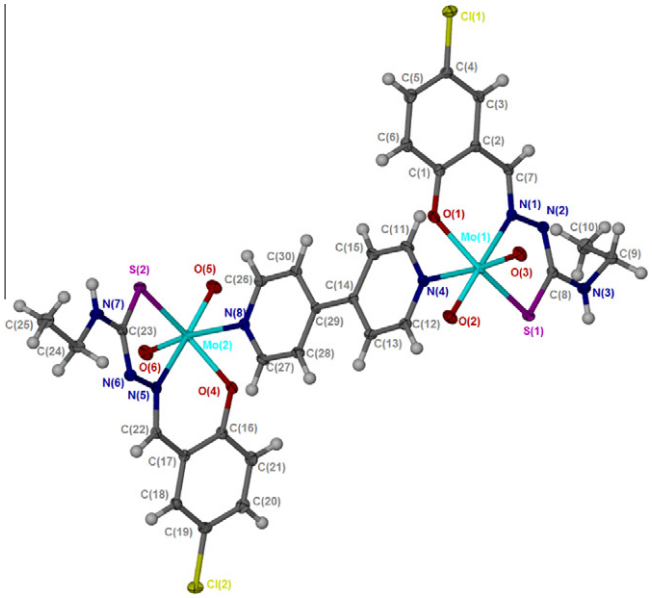

Fig. 2. ORTEP plot of **C1**, with the atom labeling scheme.

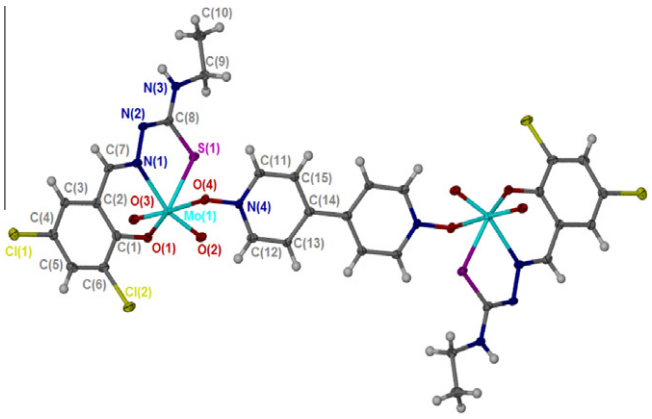

Fig. 3. ORTEP plot of **C2**, with the atom labeling scheme.

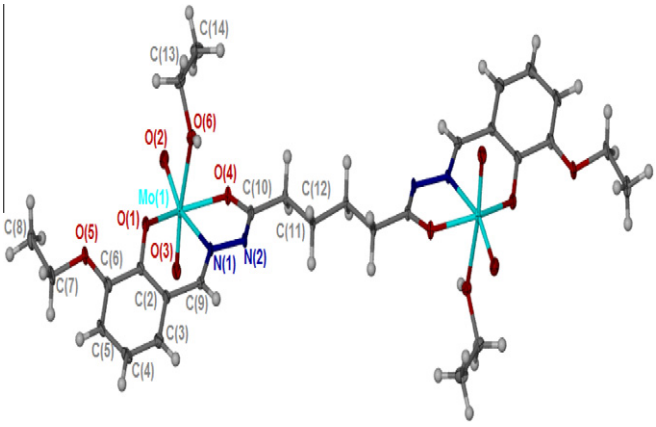

Fig. 4. ORTEP plot of **C3**, with the atom labeling scheme.

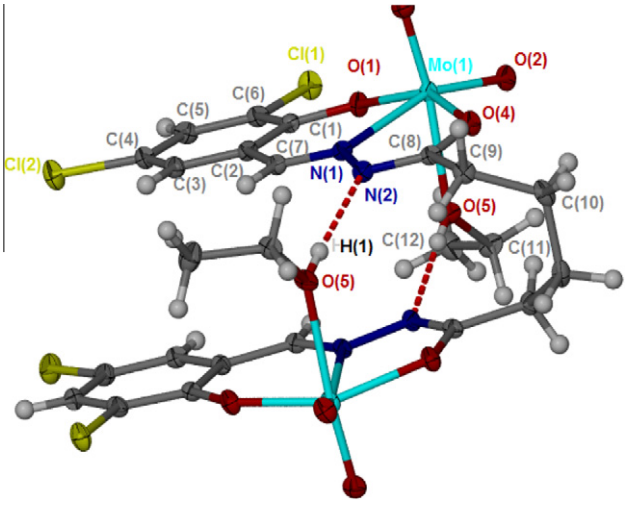

Fig. 5. ORTEP plot of **C4**, with the atom labeling scheme.

butylene chain adopts the gauche staggered conformation (Fig. 5) and Table 10. In this case, the two dioxomolybdenum fragments rotate about the C–C bond of the butylene chain to facilitate the intramolecular O–H...N hydrogen bonding between the ethanol

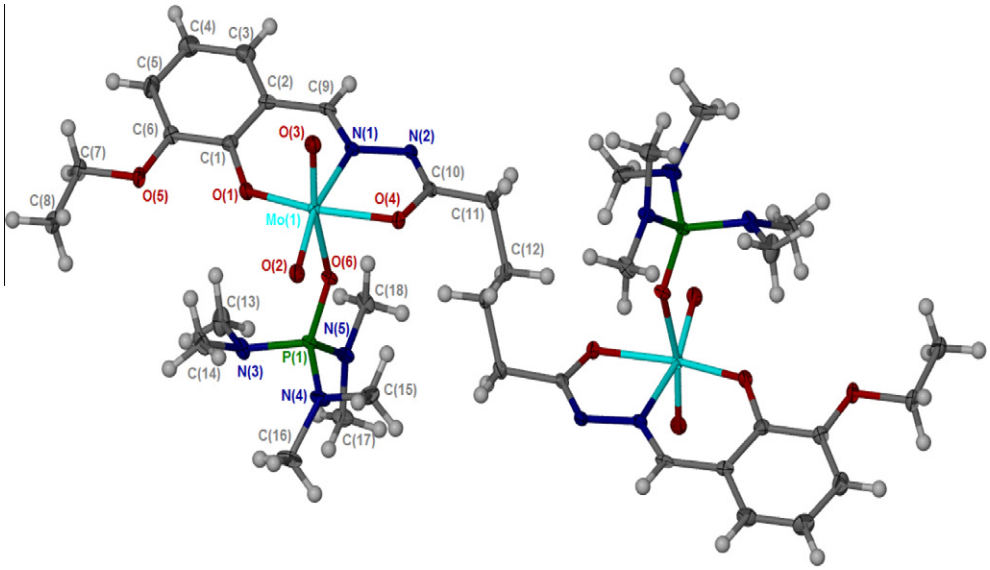

Fig. 6. ORTEP plot of **C5**, with the atom labeling scheme.

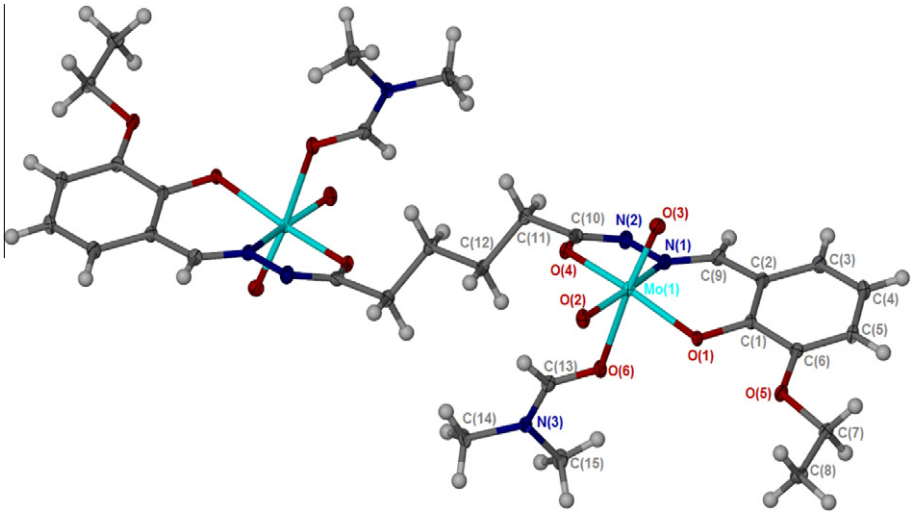

Fig. 7. ORTEP plot of **C6**, with the atom labeling scheme.

donor ligand and the imino nitrogen of the Schiff base (Fig. 13). In the case of the complex containing the ethanol molecule, **C3**, adjacent molecules are linked by OH···N hydrogen bonds into a polymeric chain that runs along the *a*-axis of the monoclinic unit cell (Fig. 14) and Table 9. Since there is no evidence of a hydrogen bonding interaction or C–H…π weak interaction in the crystal structures, **C5** and **C6** exists as discrete molecules. As shown in Fig. 15, the fundamental building block of the polymeric network in **C7** is the binuclear unit, which is linked through a covalently bonded 4,4′-bipyridine spacer group into a polymeric chain. Adjacent chains are further interconnected through an O5–H5…O2 hydrogen bond interaction, with a methanol molecule hydrogen bonded to the terminal oxygen of the molybdenum atom, leading to the formation of a two dimensional layer (Fig. 16). The layer does not appear to be flat, but is fabricated of a supramolecular staircase with the bipyridine plane (N3–C11–C12–C13–C14–C15) and the Mo1–O4–C8–N2–N4 plane lying perpendicular to one another along the *a*-axis (Fig. 17) and Table 11. The X-ray crystallographic study revealed that extensive of hydrogen bonds play a pivotal role in the self-assembly of the polymeric oxomolybdenum(VI) complexes, contributing to the supramolecular system.

3.10. Catalytic reaction of the oxomolybdenum(VI) complexes and H_2O_2 with benzyl alcohol

The oxidation of alcohol by dioxomolybdenum(VI) Schiff base complexes with H_2O_2 was carried according to the following general procedures.

10 cm^3 of benzyl alcohol (10.44 g, 0.1 mol) was mixed with 20 cm^3 of tetrahydrofuran (THF), and 0.5 g of the synthesized dioxomolybdenum(VI) complexes was added followed by 10 cm^3 of 30% H_2O_2. The mixture was kept under reflux at 90 °C for 24 h. The THF extracts were evaporated using a rotary evaporator under low pressure before treatment with Na_2SO_4. The presence of benzoic acid was detected using IR spectroscopy.

A Shidmazu Model GC 2010 Gas Chromatograph coupled with a Shidmazu GC–MS QP 2010 PLUS series mass selective and autosampler was employed for the analysis of the benzoic acid in the reaction mixture. With the help of an autoclavable digital pipette, 10 μL of the reaction mixture diluted with 10 ml of THF was prepared for GC–MS analysis. The samples were separated on a 30 mm × 0.25 mm, 0.25 μm, Rtx-5Ms silica capillary column. The column temperature was initially held at 80 °C for 1 min, then

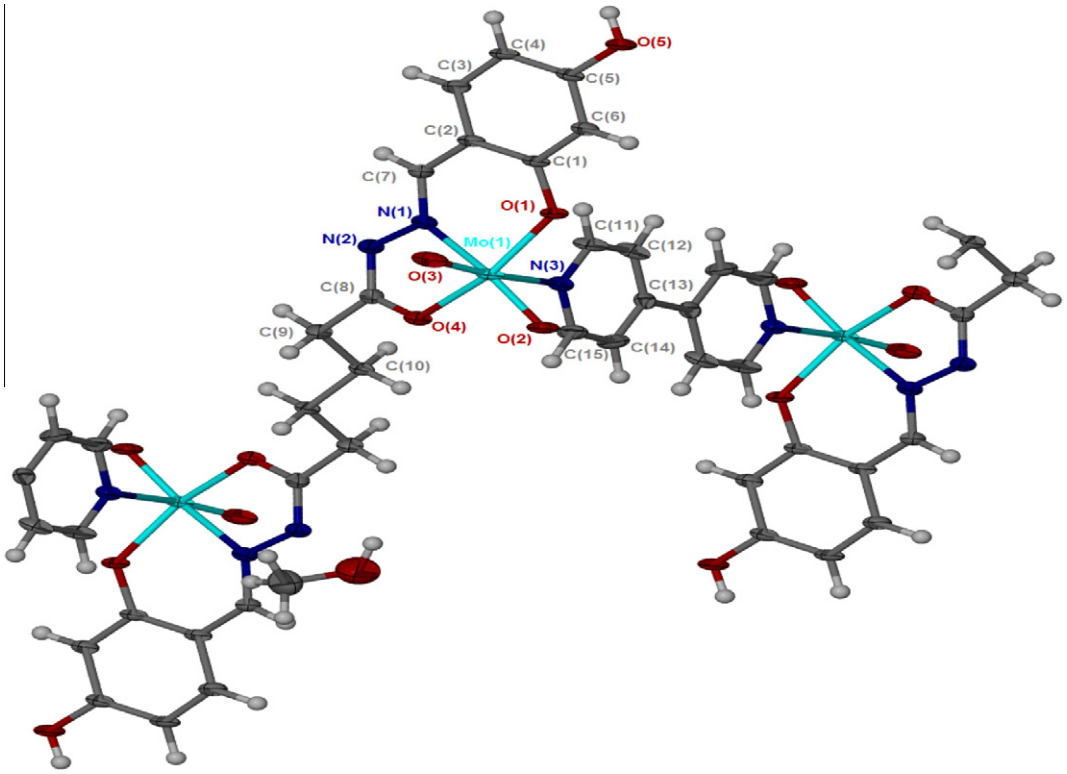

Fig. 8. ORTEP plot of **C7**, with the atom labeling scheme.

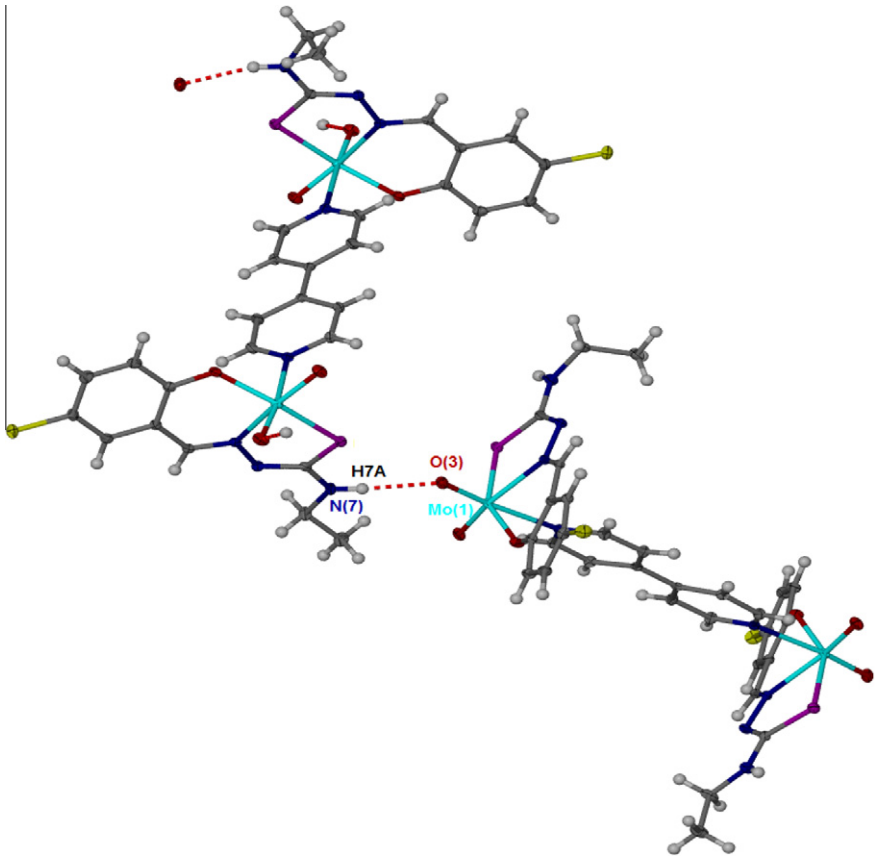

Fig. 9. Intermolecular hydrogen bond in the crystal structure of **C1**.

Table 7
Hydrogen bonds for **C1** (Å and °).

D–H...A	d(D–H)	d(H...A)	d(D...A)	∠(DHA)
N(3)–H(3)...O(6)#1	0.86	2.09	2.9278(17)	165.6
N(7)–H(7A)...O(3)#2	0.86	2.19	3.0466(16)	175.3

Symmetry transformations used to generate equivalent atoms: #1 $x + 1/2, -y + 3/2, z + ½$; #2 $x - 1/2, -y + 1/2, z - 1/2$.

Table 8
Hydrogen bonds for **C2** (Å and °).

D–H...A	d(D–H)	d(H...A)	d(D...A)	∠(DHA)
N(3)–H(3A)...O(4)#	0.86	2.21	2.959(3)	145.5

Symmetry transformations used to generate equivalent atoms: # $-x, -y + 2, -z + 2$.

the temperature was raised to 220 °C at a rate of 10 °C min^{-1}, from 220 to 280 °C at a rate of 20 °C per minute and finally held for 15 min. The total run time was 33 min. Helium gas was used as the carrier gas. The injector temperature was maintained at 300 °C and the injection volume was 1.0 μL in the splitless mode. Mass spectra were scanned from m/z 50–650 at a rate of 0.5 scan/s. The benzoic acid was identified by matching the GC retention time and mass spectra with an authentic standard. The oxidation activity was also investigated without the catalyst.

3.11. Oxidation of benzyl alcohol catalyzed by the dioxomolybdenum(VI) complexes

Oxidation reactions have been carried out using complexes **C1**–**C7** as catalysts, benzyl alcohol as a model substrate and H_2O_2 as the oxidant at 90 °C. Blank runs were performed and as expected, without catalyst, no significant benzoic acid was observed under the applied conditions, indicating the catalytic ability of the complexes. The catalytic oxidation reaction yields benzoic acid as the product only after 24 h of reaction. Additionally, the oxidation of alcohol strongly depends on the reaction temperature. At room temperature, no benzoic acid compound

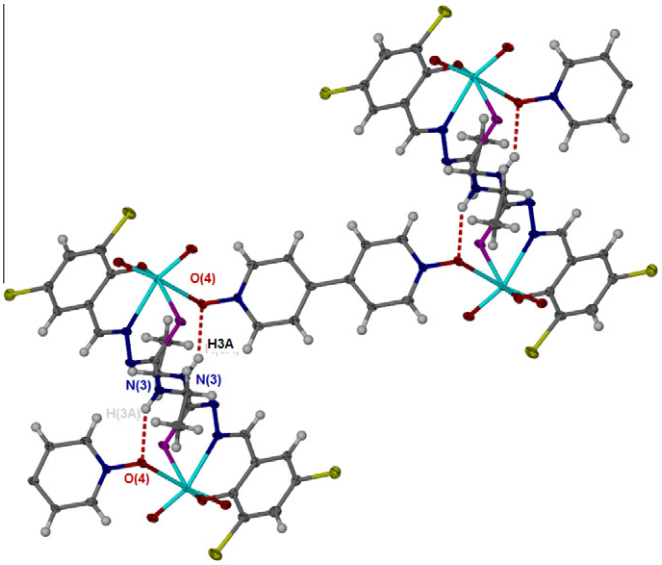

Fig. 11. Intermolecular hydrogen bond in the crystal structure of **C2**.

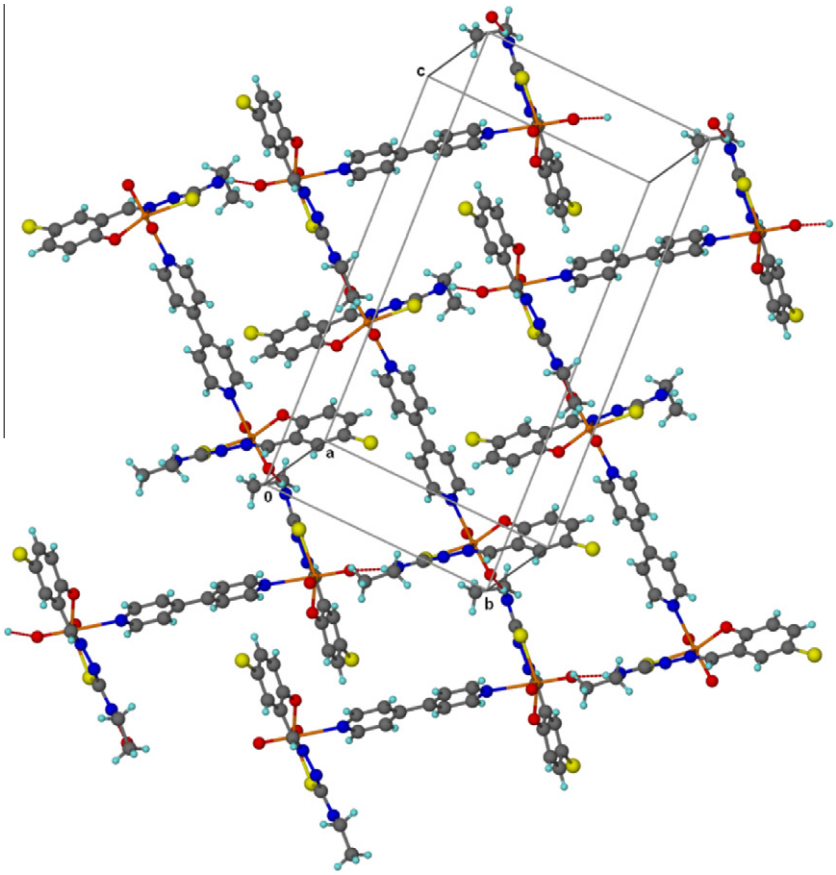

Fig. 10. Interlocking of the chain assembled by hydrogen bonding in **C1** the along the a-axis.

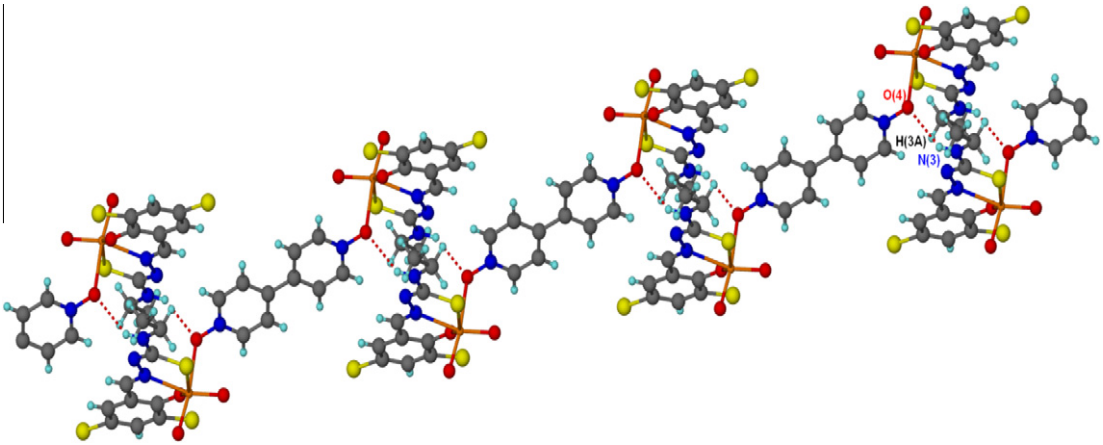

Fig. 12. X-ray crystal structure of **C2** showing the arrangement of molecules into a hydrogen bonded polymeric helical chain.

Table 9
Hydrogen bonds for **C3** (Å and °).

D–H...A	d(D–H)	d(H...A)	d(D...A)	∠(DHA)
O(6)–H(1)...N(2)#	0.62(4)	2.18(4)	2.798(3)	172(5)

Symmetry transformations used to generate equivalent atoms: # $-x, -y+1, -z+2$.

Table 10
Hydrogen bonds for **C4** (Å and °).

D–H...A	d(D–H)	d(H...A)	d(D...A)	∠(DHA)
O(5)–H(1)...N(2)#	0.70(3)	2.01(3)	2.710(2)	177(3)

Symmetry transformations used to generate equivalent atoms: # $-x+2, y, -z+½$.

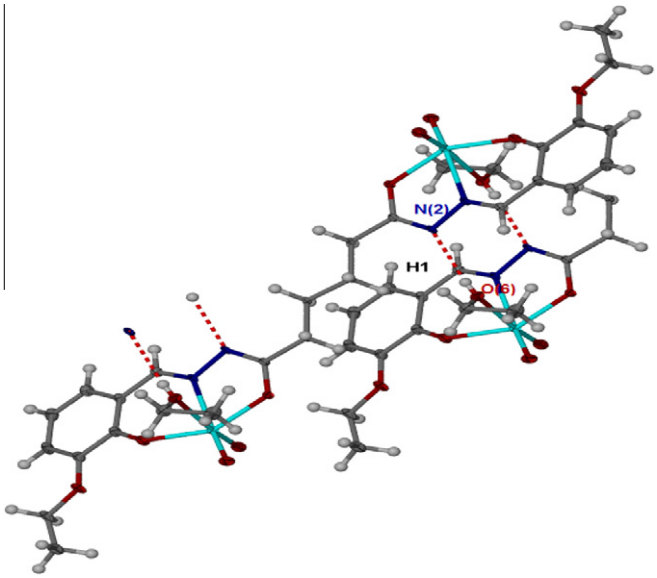

Fig. 13. Intermolecular hydrogen bond in the crystal structure of **C3**.

was observed. As we observed more than 10% conversion at 90 °C, it may be presumed that the reaction starts at a higher temperature.

As is shown in Table 12, the number of MoO_2^{2+} units in the catalyst has no major effect on the oxidation of benzyl alcohol. On the contrary, we considered the effect of the presence of the coordinating ligand in the medium of the reaction, such as 4,4-bipyridine, 4,4-bipyridine *N*,*N*′-dioxide, ethanol, HMPA and DMF.

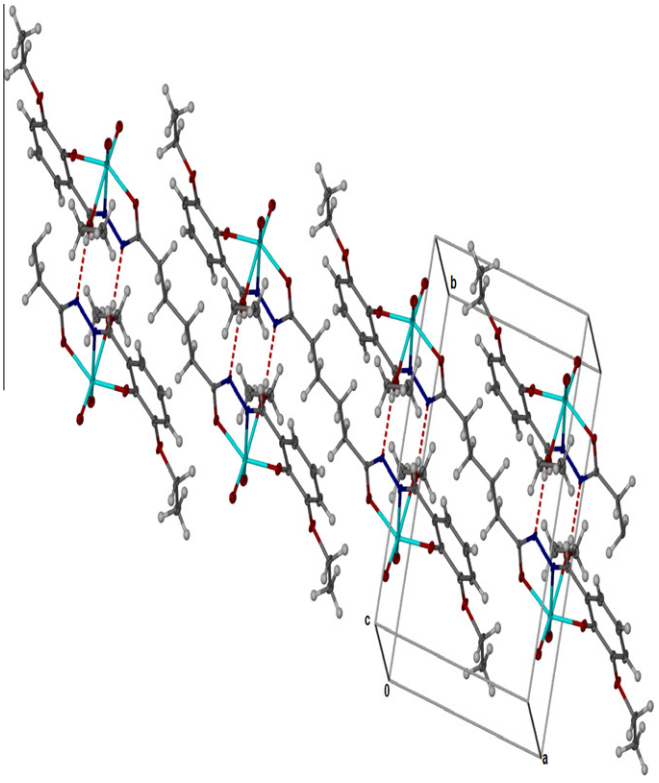

Fig. 14. Crystal structure packing of **C3**.

It can be seen that **C1** and **C7**, in which the sixth coordinating site of the Mo(VI) ion is occupied with 4,4-bipyridine as a weak bidentate ligand, show higher catalytic activity than the rest of the complexes. The reversible redox behavior, as shown by the CV analysis in this report, further support **C1** and **C7** possessing catalytic properties. According to Jia Li et al., dioxomolybdenum(VI) complexes using two connected bridging ligands containing a nitrogen donor such as 4,4′-bipyridine are found to be good catalysts for oxidation and epoxidation process using H_2O_2 as an oxidant [38]. An amine additive, such as pyridine, pyrazole and 3-cyanopyridine, enhance the efficiency of the catalytic oxidation [39–44]. The aromatic N-base ligands work by coordinating to the molybdenum center, thereby reducing the Lewis acidity of the catalyst and additionally accelerating the catalytic reaction [45,46]. It was also found that the yields of conversion by **C5** and **C6** are the lowest (Chart 1). This may be due to the

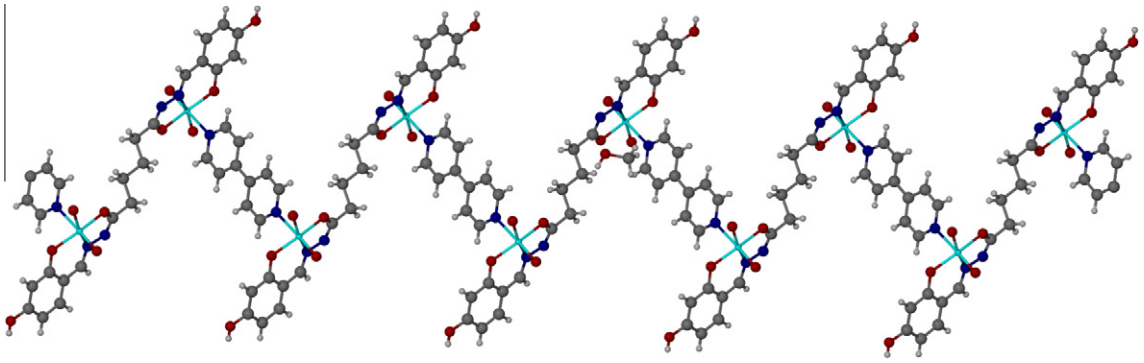

Fig. 15. ORTEP plot of **C7**.

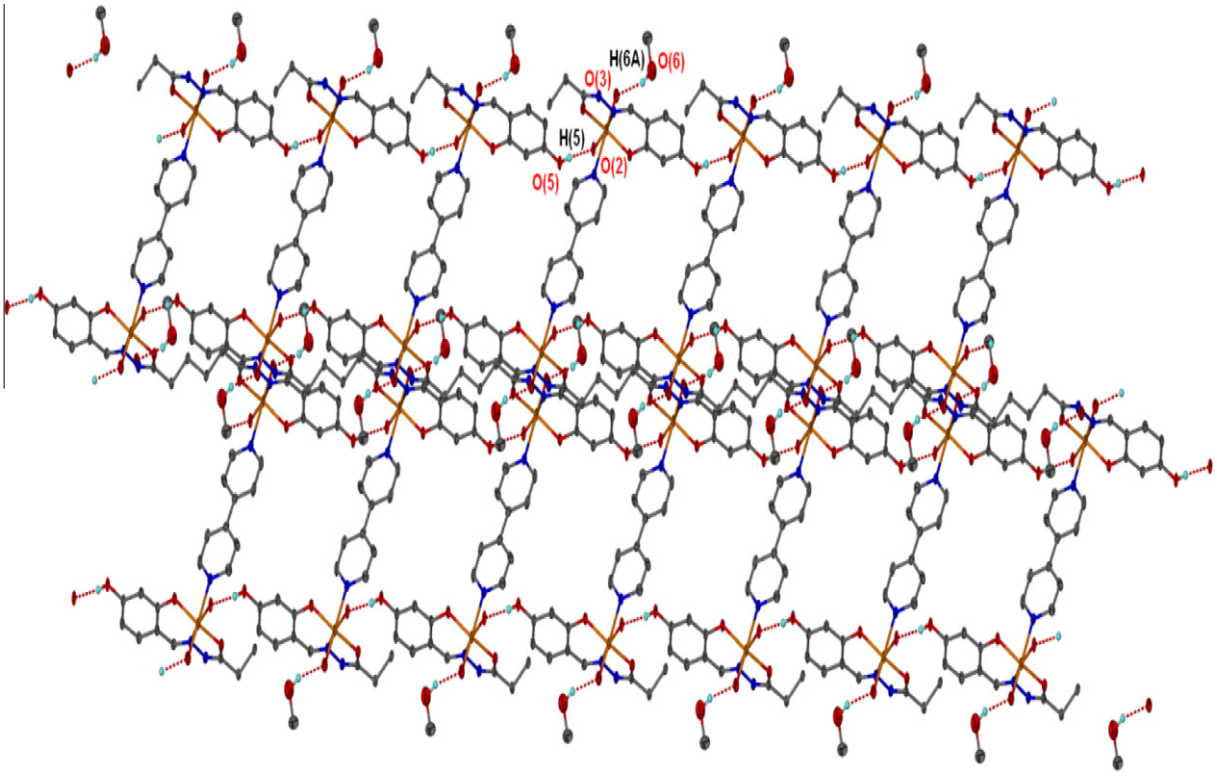

Fig. 16. Inter-chain hydrogen bonds of **C7**.

strong ability of these ligands to coordinate to the metal central, which restricts the number of free coordination sites that would be required for the catalytic oxidation of alcohols.

4. Conclusion

Several dinuclear and polynuclear dioxomolybdenum(VI) complexes have been synthesized and characterized by various physicochemical techniques and by X-ray crystallographic diffraction. In all the complexes, the structures contain two MoO_2^{2+} moieties bridged by two N atoms from bipyridine ligands or by hexadentate ligands coordinating through *ONO* atoms. The X-ray crystallographic study revealed that extensive hydrogen bonds play an important role in the self assembly of the polymeric **C1, C2, C3, C4** and **C7** complexes. The electrochemical study shows irreversible redox behavior of the *cis*-dioxomolybdenum(VI) complexes, except for **C1** and **C7**. From a catalytic property study and from CV analysis, **C1** and **C7** are found to be catalysts for oxidation reactions. Further study regarding the effect of temperature, catalyst loading and substrate concentration on the rate of oxidation reaction using dioxomolybdenum(VI) complexes will be carried out in due course.

Acknowledgment

Financial support of this work by the University of Malaya (PS378/2010B and RG020/09AFR) is greatly appreciated.

Appendix A. Supplementary data

CCDC 845679, 826697, 826694, 826696, 826695, 845680 and 825681 contain the supplementary crystallographic data for **C1**–**C7**. These data can be obtained free of charge via http://www.ccdc.cam.ac.uk/conts/retrieving.html, or from the Cambridge Crystallographic Data Centre, 12 Union Road, Cambridge CB2 1EZ, UK; fax: (+44) 1223-336-033; or e-mail: deposit@ccdc.cam.ac.uk.

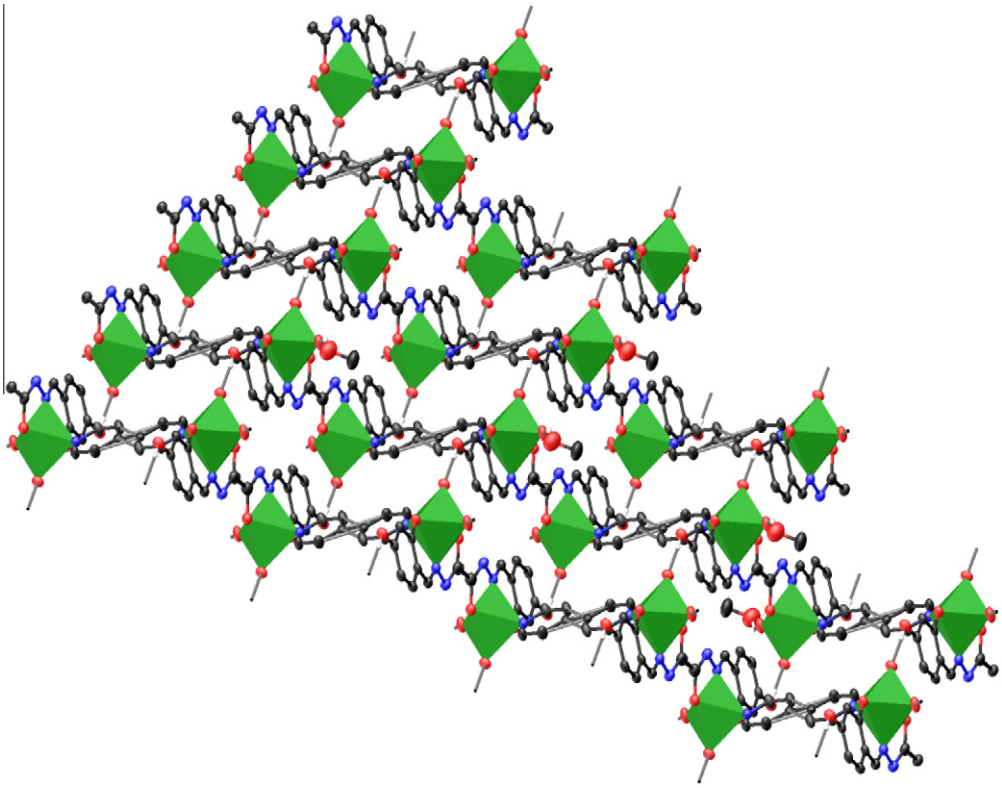

Fig. 17. Crystal packing of **C7** illustrating the formation of a supramolecular staircase (hydrogen atoms are omitted).

Table 11
Hydrogen bonds for **C7** (Å and °).

D–H...A	*d*(D–H)	*d*(H...A)	*d*(D...A)	∠(DHA)
O(5)–H(5)...O(2)#1	0.84	1.97	2.805(4)	173.6
O(6)–H(6A)...O(3)#2	0.84	2.04	2.725(6)	138.4

Symmetry transformations used to generate equivalent atoms: #1 $x-1, y, z$; #2 $x+1, y, z$.

Table 12
Screening for a suitable catalyst for the oxidation of alcohol after 24 h.

Reactants/ catalyst	Cal. mass (g)	Molar mass (g mol^{-1})	Cal. mole	Mole fraction (%)	% conversion benzyl alcohol
$C_6H_5CH_2OH$	10.40	108.14	0.10	49.80	–
H_2O_2	3.33	34.01	0.10	49.80	–
Without catalyst	–	–	–	–	0.00
Without H_2O_2	–	–	–	–	0.00
C1	0.92	923.00	0.001	0.40	26.30
C2	1.03	1026.00	0.001	0.40	12.40
C3	0.81	814.00	0.001	0.40	9.10
C4	0.87	866.00	0.001	0.40	10.30
C5	1.08	1082.00	0.001	0.40	5.50
C6	0.87	868.00	0.001	0.40	5.50
C7	0.45	445.00	0.001	0.40	40.20

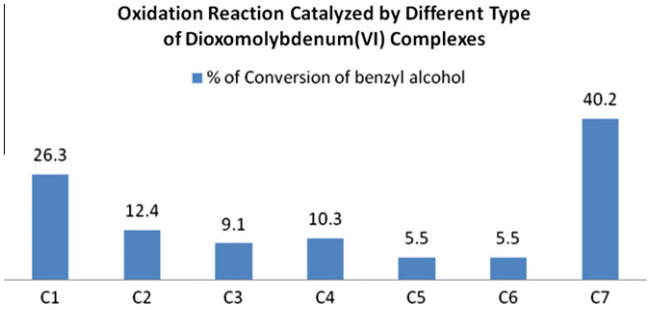

Chart 1. Oxidation reaction catalyzed by different types of dioxomolybdenum(VI) complexes. Reaction conditions: molar ratio of $C_6H_5CH_2OH/H_2O_2$ = 1:1; 0.001 mol of catalyst, temperature 90 °C for 24 h.

References

[1] B. Booth, T. Donnelly, A. Letter, Biochem. Pharmacol. 20 (1971) 3109.
[2] V.A. Kogan, L.D. Popov, V.V. Lukov, V.A. Lokshin, Zh. Neorg. Khim. 37 (1992) 2215.
[3] C. Carini, G. Pelizzi, P. Torasconi, C. Pelizzi, K.C. Molloy, P.C. Watertield, J. Chem. Soc., Dalton Trans. (1989) 289.
[4] R.D. Chakravarthy, D.K. Chand, J. Chem. Sci. 123 (2011) 187.
[5] U. Sandbhor, S. Padhye, E. Sinn, Transition Met. Chem. 27 (2002) 681.
[6] A. Syamal, M.R. Maurya, Transition Met. Chem. 11 (1986) 235.
[7] S.N. Rao, K.N. Munshi, N.N. Rao, M.M. Bahdbhade, E. Suresh, Polyhedron 18 (1999) 2491.
[8] D.W. Kim, U. Lee, B.K. Koo, Bull. Korean Chem. Soc. 25 (2004) 1071.
[9] M. Cindric, V. Vrdoljak, N. Strukan, B. Kamenar, Polyhedron 24 (2005) 369.
[10] E.Z. Iveges, V.M. Leovac, G. Pavlovic, M. Penavic, Polyhedron 11 (1992) 1659.
[11] J. Liimatainen, A. Lehtonen, R. Sillanpaa, Polyhedron 19 (2000) 1133.
[12] F.J. Arnaiz, R. Aguado, M.R. Pedrosa, A.D. Cian, J. Fischer, Polyhedron 19 (2000) 2141.
[13] C.S. Marvel, N. Tarkoy, J. Am. Chem. Soc. 79 (1957) 6000.
[14] R. Dinda, S. Ghosh, L.R. Falvello, M. Tomas, T.C.W. Mak, Polyhedron 25 (2006) 2375.
[15] B.K. Koo, H. Kang, W.T. Lim, Bull. Korean Chem. Soc. 29 (2008) 1819.
[16] M.M. Jones, J. Am. Chem. Soc. 81 (1959) 3188.
[17] G.M. Shedrick, Acta Crystallogr., Sect. A 64 (2008) 112.
[18] S.A. Attia, S.F. El-Mashtloy, M.F. El-Shabbat, Polyhedron 22 (2003) 895.
[19] M. Kato, K. Najikama, T. Yoshikawa, M. Hirothsu, M. Kojima, Inorg. Chim. Acta 311 (2000) 619.
[20] E.I. Stiefel, Prog. Inorg. Chem. 22 (1977) 1.

[21] R. Dinda, P. Sengupta, S. Ghosh, W.S. Sheldrick, Eur. J. Inorg. Chem. (2003) 363. and references there in.
[22] S.S. Singh, C.B.S. Sengar, Indian J. Chem. 7 (1969) 812.
[23] S.M. Horner, S.Y. Tyree, Inorg. Chem. 1 (1962) 122.
[24] N.M. Karayannis, L.L. Pytlewski, C.M. Mikulski, Coord. Chem. Rev. 11 (1973) 93.
[25] R.G. Garvey, J.H. Nelson, R.O. Ragsdale, Coord. Chem. Rev. 3 (1968) 375.
[26] W. Kemp, Organic Spectroscopy, third ed., Palgrave Publisher, 1991.
[27] B. Ji, Q. Du, K. Ding, Y. Li, Z. Zhou, Polyhedron 15 (1996) 403.
[28] H.A. El-Boraey, J. Therm. Anal. Calorim. 81 (2005) 339.
[29] K.R. Surati, B.T. Thaker, J. Coord. Chem. 94 (1) (2008) 247.
[30] L.M. Fostiak, I. Garcia, J.K. Swearingen, E. Bermejo, A. Castineiras, D.X. West, Polyhedron 22 (2003) 83.
[31] J.H. Enemark, C.G. Young, Adv. Inorg. Chem. 40 (1993) 1.
[32] A. Rana, R. Dinda, P. Sengupta, S. Ghosh, I.R. Falvello, Polyhedron 21 (2002) 1023.
[33] C. Bustos, O. Burckhardt, R. Schrebler, D. Corrillo, A.M. Arif, A.H. Cowley, C.M. Nunn, Inorg. Chem. 29 (1990) 3996.
[34] K.B. Bernard, M. Bruck, S. Huber, C. Grittini, J.H. Enemark, R.W. Gable, A.G. Wedd, Inorg. Chem. 36 (1997) 637.
[35] C.S.J. Chang, J.H. Enemark, Inorg. Chem. 30 (1991) 683.
[36] A.S. Attia, S.F. El-Mashtoly, M.F. El-Shahat, Polyhedron 22 (2003) 895.
[37] S. Purohit, A. Koley, P. Prasad, P.T. Manoharan, S. Ghosh, Inorg. Chem. 28 (1989) 3735.
[38] Y. Luan, G. Wang, R.L. Lick, M. Yang, Eur. J. Inorg. Chem. 9 (2007) 1215.
[39] J. Rudolph, K.L. Reddy, J.P. Chiang, K.B. Sharpless, J. Am. Chem. Soc. 119 (1997) 6189.
[40] W.A. Herrmann, H. Ding, R.M. Kratzer, F.E. Kuhn, J.J. Haider, R.W. Fischer, J. Organomet. Chem. 549 (1997) 319.
[41] W.A. Herrmann, R.M. Kratzer, H. Ding, W.R. Thiel, H. Glass, J. Organomet. Chem. 555 (1998) 293.
[42] C. Coperet, H. Adolfsson, K.B. Sharpless, Chem. Commun. (1997) 1565.
[43] H. Adolfsson, A. Converso, K.B. Sharpless, Tetrahedron Lett. 40 (1999) 3991.
[44] H. Adolfsson, A. Converso, J.P. Chiang, A.K. Yudin, J. Organomet. Chem. 65 (2000) 8651.
[45] F.E. Kuhn, A.M. Santos, P.W. Roesky, E. Herdtweck, W. Scherer, P. Gisdakis, I.V. Yudanov, C. Di Valentin, N. Rosch, Chem. Eur. J. 5 (1999) 3603.
[46] P. Ferreira, W.M. Xue, E. Bencze, E. Herdweck, F.E. Kuhn, Inorg. Chem. 40 (2001) 5834.